© 2021. Published by The Company of Biologists Ltd | Journal of Cell Science (2021) 134, jcs249193. doi:10.1242/jcs.249193

RESEARCH ARTICLE

The 5-HT$_4$ receptor interacts with adhesion molecule L1 to modulate morphogenic signaling in neurons

Simon Bennet Sonnenberg[1], Jonah Rauer[1], Christoph Göhr[1], Nataliya Gorinski[1], Sophie Kristin Schade[1], Dalia Abdel Galil[1], Vladimir Naumenko[2], André Zeug[1], Stephan C. Bischoff[3], Evgeni Ponimaskin[1,2,4,*] and Daria Guseva[1,3,*]

ABSTRACT

Morphological remodeling of dendritic spines is critically involved in memory formation and depends on adhesion molecules. Serotonin receptors are also implicated in this remodeling, though the underlying mechanisms remain enigmatic. Here, we uncovered a signaling pathway involving the adhesion molecule L1CAM (L1) and serotonin receptor 5-HT$_4$ (5-HT$_4$R, encoded by *HTR4*). Using Förster resonance energy transfer (FRET) imaging, we demonstrated a physical interaction between 5-HT$_4$R and L1, and found that 5-HT$_4$R–L1 heterodimerization facilitates mitogen-activated protein kinase activation in a G_s-dependent manner. We also found that 5-HT$_4$R–L1-mediated signaling is involved in G_{13}-dependent modulation of cofilin-1 activity. In hippocampal neurons *in vitro*, the 5-HT$_4$R–L1 pathway triggers maturation of dendritic spines. Thus, the 5-HT$_4$R–L1 signaling module represents a previously unknown molecular pathway regulating synaptic remodeling.

KEY WORDS: Serotonin receptor 5-HT$_4$, Adhesion molecule L1, Heterodimerization, ERK phosphorylation, Cofilin-1 activity, Spine formation

INTRODUCTION

Understanding the molecular mechanisms regulating neuronal morphology and synaptogenesis is a central point in studies investigating potential strategies for the treatment of neurological and psychiatric diseases. One of the signaling molecules critically involved in neurogenesis, neurite outgrowth, dendritic spine formation and synaptic plasticity is serotonin, or 5-hydroxytryptamine (5-HT). Serotonin operates through the activation of a heterogeneous group of specific 5-HT receptors with different functions (Herr et al., 2017; Mawe and Hoffman, 2013; Müller and Cunningham, 2020; Wirth et al., 2017). One of these receptors, serotonin receptor 5-HT$_4$ (5-HT$_4$R, encoded by *HTR4*), is known to regulate learning and memory, and is also involved in several neurological disorders (Eglen et al., 1995; Johnson et al., 2012; Lo et al., 2014; Lucas et al., 2007; Marchetti et al., 2011). The 5-HT$_4$R is a seven transmembrane domain receptor that exerts its effects through coupling to the heterotrimeric G_s protein, which activates adenylyl cyclase, inducing an increase in cAMP levels and subsequent increase in phosphorylation of downstream effectors mediated by ERK (ERK1 and ERK2, also known as MAPK3 and MAPK1) (Bockaert et al., 1990; Heine et al., 2002; Norum et al., 2003). We have also shown that the 5-HT$_4$R is coupled to G_{13} proteins to activate the small GTPase RhoA, leading to changes in cellular morphology and spine maturation via modulation of cofilin phosphorylation and actin polymerization (Ponimaskin et al., 2002; Schill et al., 2020). Several studies have suggested that the functions of the 5-HT$_4$R may be regulated through receptor homo-oligomerization (Pellissier et al., 2011), or through hetero-oligomerization with other G-protein-coupled receptors (GPCRs) (Berthouze et al., 2005). However, no published investigations have demonstrated an interaction of the 5-HT$_4$R with non-GPCR proteins (e.g. cell adhesion molecules or cellular matrix proteins) known to modulate the cytoskeleton and/or cellular morphology.

One of the cell adhesion molecules critically involved in neuronal migration, axonal development, growth cone formation, guidance of axons and synaptic plasticity is the adhesion molecule L1CAM (L1; Luthi et al., 1996; Maness and Schachner, 2007; Patzke et al., 2016; Sytnyk et al., 2017). L1 is also beneficial for repair processes in the adult central nervous system (CNS) of vertebrates by promoting axonal growth and neuronal survival (Chen et al., 2007; Roonprapunt et al., 2003; Zhang et al., 2005). L1 mutations have been found in certain forms of X-linked mental retardation (Kenwrick et al., 2000), and polymorphisms in the L1 gene are associated with schizophrenia in some populations (Frints et al., 2003; Kurumaji et al., 2001). L1 can also contribute to stress-related mood disorders and depression in humans, as well as animal models of depression (Laifenfeld et al., 2005; Sandi and Bisaz, 2007). Similar to the 5-HT$_4$R, the role of L1 in the regulation of neuronal morphology has been demonstrated by L1-dependent cofilin phosphorylation and neurite outgrowth (Figge et al., 2012). In addition, L1-mediated ERK activation after the application of function-triggering antibodies to L1 may be important for the regulation of neuronal cell functions (Schmid et al., 2004). L1 consists of six immunoglobulin (Ig) domains, five fibronectin type III domains, a single transmembrane region and an intracellular domain (Moos et al., 1988). The second Ig domain, but not the cytoplasmic domain, has been shown to be involved in homophilic binding (Hortsch et al., 1995; Wong et al., 1995; Zhao and Siu, 1995). L1 can operate as a heterophilic binding partner with FGF, other cell adhesion molecules (CAMs), integrins and proteoglycans, and this interaction is involved in neurite extension and axonal growth (DeBernardo and Chang, 1996; Doherty and Walsh, 1996; Gibson, 2011; Hall et al., 2004; Hortsch et al., 2009; Milev et al., 1994; Schmid and Maness, 2008). However, the mechanisms underlying signaling transduction are not fully understood.

[1]Department of Cellular Neurophysiology, Hannover Medical School, Hannover 30625, Germany. [2]Institute of Cytology and Genetics of the Siberian Branch of the Russian Academy of Sciences, Novosibirsk 630090, Russia. [3]Department of Nutritional Medicine, University of Hohenheim, Stuttgart 70599, Germany. [4]Institute of Neuroscience, Lobachevsky State University of Nizhny Novgorod, Nizhny Novgorod 603950, Russian Federation.

*Authors for correspondence (daria.guseva@uni-hohenheim.de; ponimaskin.evgeni@mh-hannover.de)

S.B.S., 0000-0002-2782-796X; J.R., 0000-0001-9336-1048; C.G., 0000-0002-9377-4579; N.G., 0000-0002-5606-7162; S.K.S., 0000-0002-8060-8213; V.N., 0000-0001-7196-4729; E.P., 0000-0002-4570-5130; D.G., 0000-0002-8844-572X

Handling Editor: Giampietro Schiavo
Received 22 May 2020; Accepted 19 January 2021

Journal of Cell Science (2021) 134, jcs249193. doi:10.1242/jcs.249193

In the present study, we demonstrated that the 5-HT$_4$R physically interacts with L1, and this interaction facilitates receptor-mediated phosphorylation of ERK in a Gα_s-dependent manner. We also demonstrated that 5-HT$_4$R–L1-mediated signaling is involved in the modulation of cofilin-1 phosphorylation and receptor-dependent spine maturation in hippocampal neurons.

RESULTS

5-HT$_4$R and L1 physically interact at the plasma membrane of HEK cells

We analyzed the interaction between the 5-HT$_4$R and L1 at the cell membrane of transfected living HEK cells, which do not express endogenous 5-HT$_4$R and L1, allowing us to observe the interaction of the recombinant proteins without significant involvement of endogenous proteins using the Förster resonance energy transfer (FRET) approach. We measured FRET occurrence between 5-HT$_4$R–mTurquoise2 (mTq2) (donor) and L1–YPet (acceptor) using the linear unmixing (lux)-FRET method (Wlodarczyk et al., 2008). Confocal microscopic analysis revealed that 5-HT$_4$R–mTq2 and L1–YPet colocalized at the plasma membrane of HEK cells (Fig. 1A), where they were expressed at similar concentrations, as indicated by the donor molar fraction, x_D, in the range of 0.5 (Fig. S1). The lux-FRET analysis indicated high apparent FRET efficiency (Ef_{DA}) for 5-HT$_4$R–mTq2 and L1–YPet (18.4%±0.2%, mean±s.e.m.; Fig. 1B,C), suggesting a specific interaction between these proteins. As a negative control, we used CD86 protein

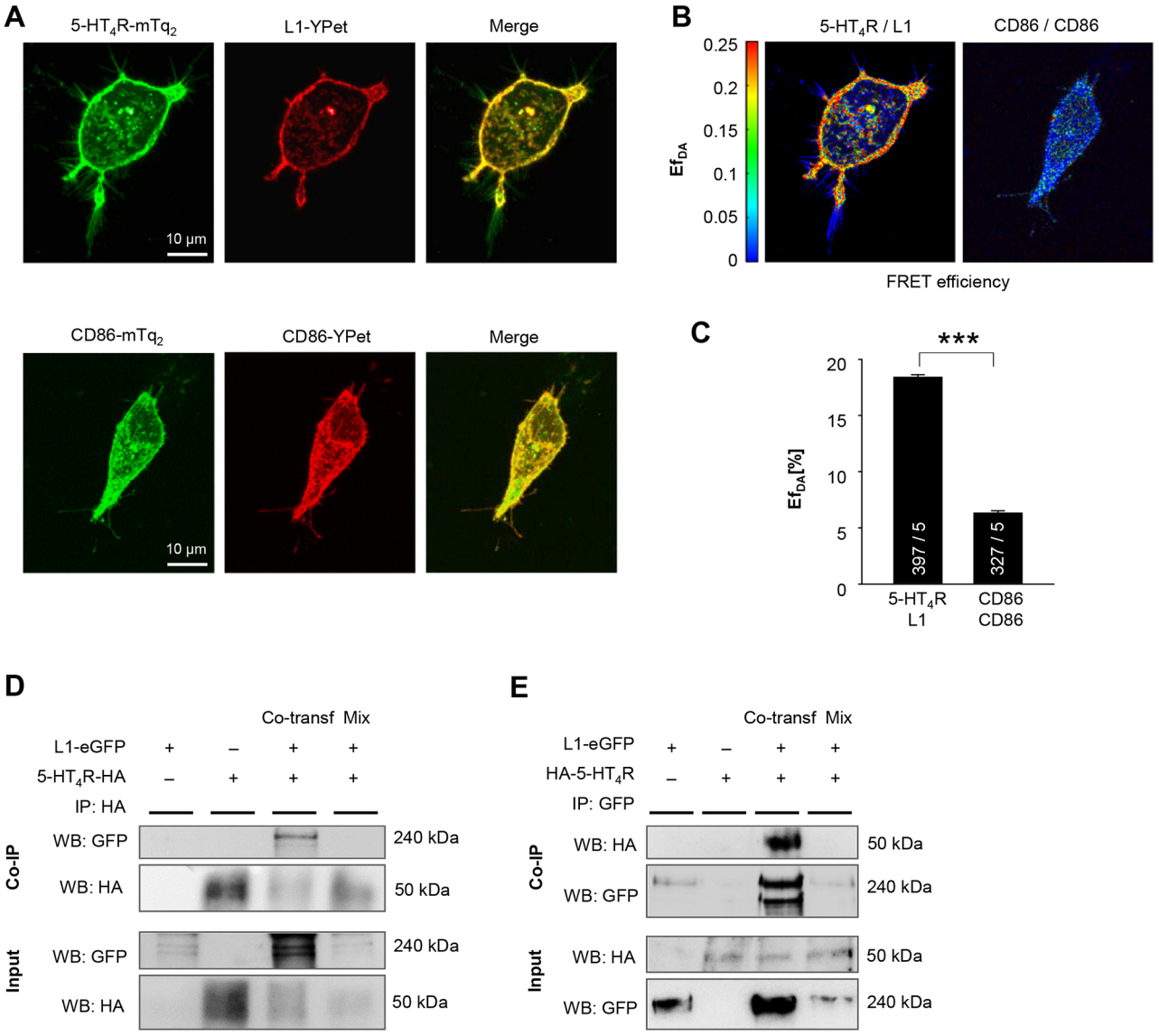

Fig. 1. The 5-HT$_4$R and L1 interact directly at the plasma membrane of transfected HEK cells. (A) Distribution of 5-HT$_4$R–mTq2 and L1–Ypet (upper panel), CD86–mTq2 and CD86–Ypet (lower panel), and a merged image calculated by linear unmixing of the fluorescence emission spectra. (B) The representative cells from A, showing apparent FRET efficiency (Ef_{DA}) between 5-HT$_4$R–mTq2 and L1–Ypet (left), and no FRET appearance between CD86–mTq2 and CD86–Ypet (right). (C) Quantitative analysis of FRET efficiencies between 5-HT$_4$R–mTq2 and L1–Ypet (Ef_{DA}=18.4%±0.2%), and between CD86–mTq2 and CD86–YPet (Ef_{DA}=6.3%±0.2%). Data are presented as mean±s.e.m. The *n* is indicated in the bars and represents the total number of cells/total number of independent cultures. ***P<0.001 (unpaired, two-tailed Student's *t*-test). (D,E) Co-IP experiments of recombinant 5-HT$_4$R–HA and L1–eGFP in HEK cells. Top: expression of proteins after immunoprecipitation (Co-IP). Bottom: expression of proteins before immunoprecipitation (Input; 5% of total lysate). Co-transf, lysates from co-transfected cells; Mix, mixed lysates from singly transfected cells; WB, western blot. Representative images from at least four independent experiments.

Journal of Cell Science (2021) 134, jcs249193. doi:10.1242/jcs.249193

(Fig. 1A), which is known to be a monomer at the plasma membrane (Van Gijsegem et al., 2008). The Ef_{DA} between CD86–mTq2 and CD86–YPet was 6.3%±0.2% (Fig. 1B,C).

The interaction between the 5-HT$_4$R and L1 was further confirmed by co-immunoprecipitation (co-IP) experiments using plasma membrane fractions isolated from HEK cells co-transfected with 5-HT$_4$R–HA and L1–eGFP. After immunoprecipitation with an anti-HA antibody, the eGFP signal was detected only in samples derived from cells co-expressing 5-HT$_4$R–HA and L1–eGFP (Fig. 1D). In addition to the full-length L1–eGFP (~227 and 247 kDa, corresponding to the phosphorylated and non-phosphorylated forms of L1, respectively), we observed a band of ~107 kDa, which corresponds to the membrane-spanning C-terminal 80 kDa L1 fragment (L1-80 kDa) tagged with eGFP (Fig. S3A). In contrast to input lysates, there were neither C-terminal 32 kDa (L1-32 kDa) nor 28 kDa (L1-28 kDa) fragments of L1 (i.e. 59 kDa and 55 kDa fragments, respectively, when tagged with eGFP) detectable after precipitation with anti-HA antibody (Fig. S3A). Notably, in mixed lysates from cells after single transfection with 5-HT$_4$R–HA or L1–eGFP, no co-IP was detected (Fig. 1D, Mix), indicating an absence of artificial protein interaction because of overexpression. In addition, no eGFP signal was detectable after transfection with 5-HT$_4$R–HA or L1–eGFP alone. Similar results were obtained after immunoprecipitation with anti-GFP antibody followed by western blotting using an antibody against the HA tag; the HA signal was identified only in samples derived from cells co-expressing 5-HT$_4$R–HA and L1–eGFP (Fig. 1E). Taken together, the results of the lux-FRET analysis and co-IP experiments suggested a physical interaction between the 5-HT$_4$R, full-length L1 and L1-80 kDa at the plasma membrane.

Co-expression of L1 facilitates 5-HT$_4$R-mediated ERK activation in a Gα_s-dependent manner

Activation of 5-HT$_4$R has previously been demonstrated to result in increased ERK phosphorylation in transfected HEK293 cells (Barthet et al., 2007). To verify the role of the 5-HT$_4$R–L1 interaction in ERK phosphorylation, we incubated the lysates of HEK cells co-transfected with 5-HT$_4$R–mCherry and L1–eGFP with antibodies against phosphorylated ERK (pERK) or ERK. Expression of L1 alone did not modulate ERK activation, whereas cells transfected with the 5-HT$_4$R exhibited increased ERK phosphorylation upon receptor stimulation with the 5-HT$_4$R agonist BIMU8 (pERK:ERK ratio 21.2±2.6, mean±s.e.m.; Fig. 2A,B). Co-expression of the receptor with L1 led to significant facilitation of BIMU8-mediated ERK activation (pERK:ERK ratio 47.9±5.1; Fig. 2A,B). This response was 5-HT$_4$R-dependent because it was completely blocked by pre-treatment with the selective receptor antagonist GR113808. In control experiments (pcDNA), we did not detect any changes in ERK phosphorylation upon BIMU8 treatment (Fig. 2A, B). These results suggest that the interaction between the 5-HT$_4$R and L1 facilitates receptor-mediated signaling towards ERK activation. Notably, co-expression of 5-HT$_4$R and L1 induced the appearance of L1-32 kDa and L1-28 kDa fragments (detectable as bands with molecular weight of 59 kDa and 55 kDa; Fig. S3B) compared to the L1 expression alone.

To better understand the underlying molecular mechanisms, we evaluated the possible implication of the heterotrimeric G$_s$ protein, a canonical downstream effector of the 5-HT$_4$R (Ponimaskin et al., 2002). We developed a set of specific shRNAs that highly selectively knocked down Gα_s expression (Fig. S2A,B). To test whether Gα_s plays a role in increased ERK phosphorylation after co-expression of the 5-HT$_4$R and L1, we compared ERK activation in cells expressing 5-HT$_4$R alone or co-expressing 5-HT$_4$R and L1, paralleled by silencing of Gα_s using shRNA. In this experiment, we also observed L1-80 kDa and L1-32 kDa fragments (Fig. S4A), although the appearance of the L1-32 kDa fragment was not so pronounced as in experiments without shRNA application (Fig. S3A,B). Western blot analysis revealed that, in experiments using cells transfected with 5-HT$_4$R and shRNA against Gα_s, treatment with BIMU8 still resulted in a significant increase in ERK phosphorylation (Fig. 3). This

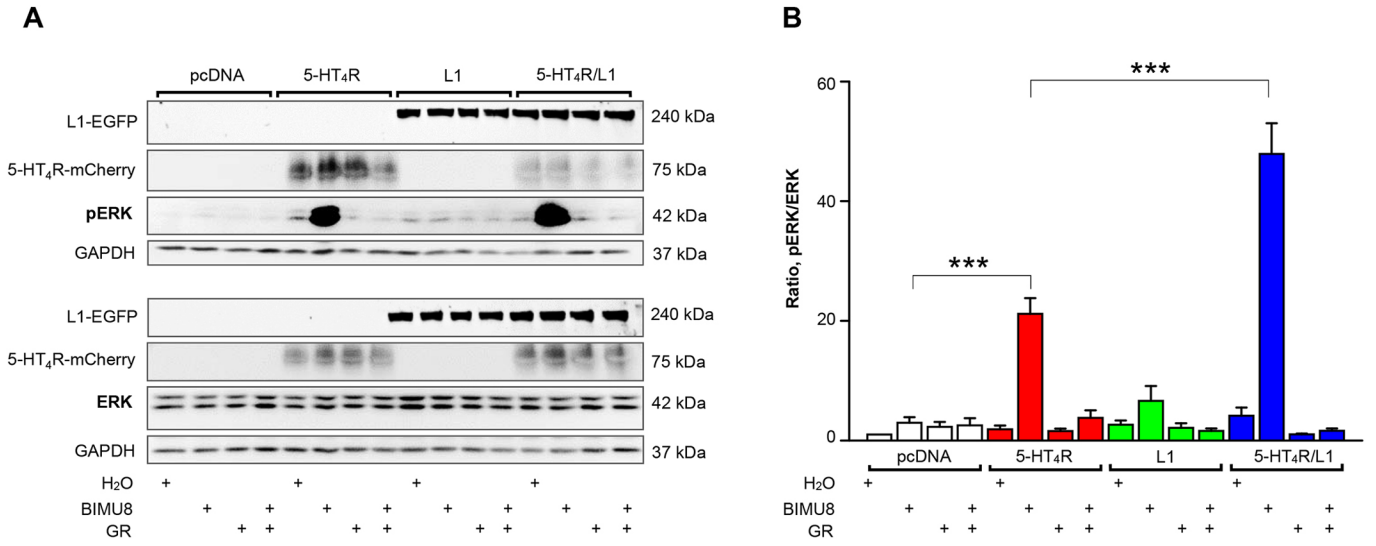

Fig. 2. Interaction between the 5-HT$_4$R and L1 increases ERK phosphorylation in transfected HEK cells. (A) HEK cells transfected with control vector (pcDNA), 5-HT$_4$R–mCherry (5-HT$_4$R), L1–eGFP (L1), or both 5-HT$_4$R–mCherry and L1–eGFP (5-HT$_4$R/L1) were treated with BIMU8 (5-HT$_4$R agonist) and/or GR113808 (GR; 5-HT$_4$R antagonist), or with water as a vehicle control, and lysates were blotted for the indicated proteins. GAPDH is shown as a loading control. In HEK cells co-transfected with 5-HT$_4$R–mCherry and L1–eGFP, application of BIMU8 leads to a 2-fold increase in ERK phosphorylation (pERK) compared to HEK cells with a single 5-HT$_4$R transfection. (B) Quantitative analysis of pERK:ERK ratio in western blotting experiments. Data are presented as mean±s.e.m. (n=4). ***P<0.001 (two-way ANOVA with Tukey's post hoc test).

Journal of Cell Science (2021) 134, jcs249193. doi:10.1242/jcs.249193

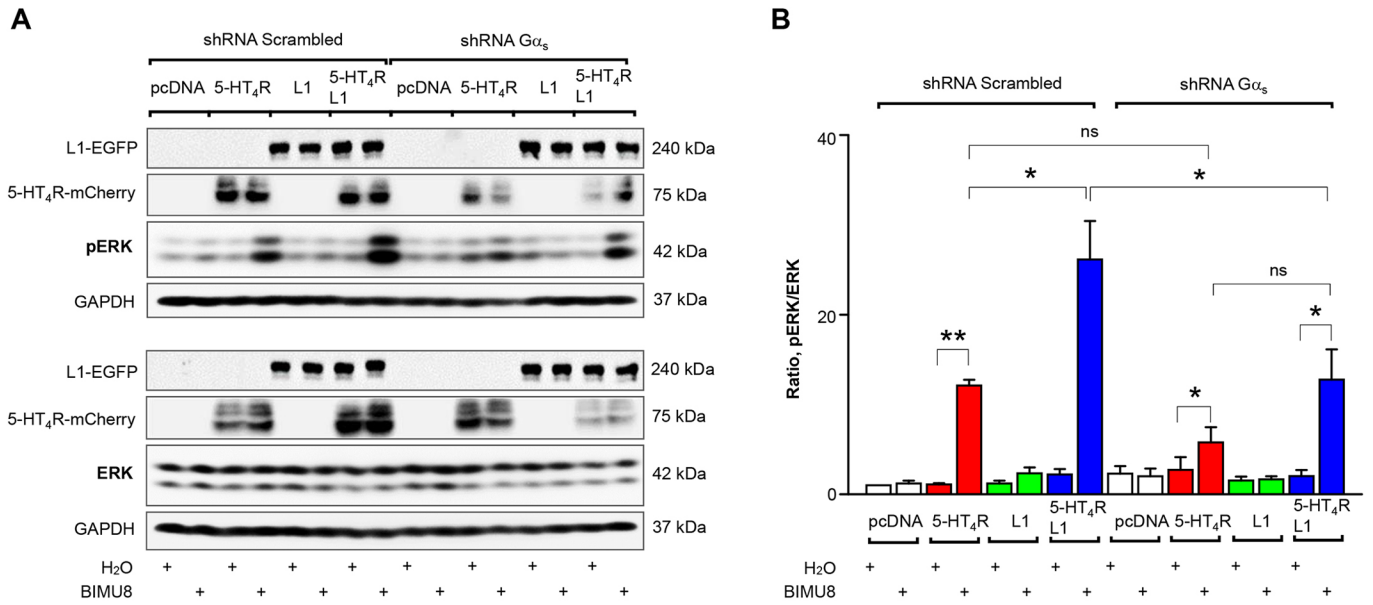

Fig. 3. Interaction between the 5-HT$_4$R and L1 induces an increase in ERK phosphorylation via Gα$_s$. (A) HEK cells transfected with control vector (pcDNA), 5-HT$_4$R–mCherry (5-HT$_4$R), L1–eGFP (L1), or both 5-HT$_4$R–mCherry and L1–eGFP (5-HT$_4$R/L1) were treated with BIMU8 (5-HT$_4$R agonist) or with water as a vehicle control, and lysates were blotted for the indicated proteins. GAPDH is shown as a loading control. In HEK cells co-transfected with 5-HT$_4$R and L1, treatment with BIMU8 leads to increased ERK phosphorylation (pERK). This effect is significantly reduced by shRNA against Gα$_s$ (shRNA Gα$_s$). Non-targeting shRNA was used as a control (shRNA scrambled). (B) Quantitative analysis of pERK:ERK ratio in western blotting experiments. Data are presented as mean±s.e.m. (*n*=3). **P*<0.05; ***P*<0.01; ns, not significant (two-way ANOVA with Tukey's post hoc test).

observation is in line with earlier studies showing that the 5-HT$_4$R activates the ERK pathway in a G$_s$–cAMP–PKA-independent manner (Barthet et al., 2007). More importantly, silencing of Gα$_s$ significantly reduced the ERK phosphorylation mediated by BIMU8 in cells co-expressing 5-HT$_4$R–L1 compared to that in cells co-transfected with scrambled shRNA (Fig. 3A,B). This finding suggests that, in the case of the 5-HT$_4$R–L1 interaction, the Gα$_s$ subunit may be recruited as an additional downstream effector regulating ERK phosphorylation.

Interaction between the 5-HT$_4$R and L1 modulates cofilin-1 phosphorylation

The 5-HT$_4$R activates the heterotrimeric G$_{13}$ protein, resulting in RhoA-dependent neurite retraction and cell rounding under basal conditions and after agonist stimulation (Ponimaskin et al., 2002). Moreover, our recent study provided evidence that the 5-HT$_4$R–G$_{13}$–RhoA signaling cascade stimulates phosphorylation of the actin-binding protein cofilin in neuroblastoma N1E-115 cells, as well as in neurons (Schill et al., 2020).

To study the role of the 5-HT$_4$R–L1 interaction in G$_{13}$-mediated cofilin phosphorylation, we developed a set of specific shRNAs that highly selectively knocked down expression of Gα$_{13}$ (Fig. S2C,D). Similarly to results obtained in experiments with shRNA targeting Gα$_s$, we obtained the full-length L1, along with L1-80 kDa fragments and a weak band corresponding to the L1-32 kDa fragment (Fig. S4B). In control experiments (scrambled shRNA), BIMU8 stimulation of the 5-HT$_4$R expressed either alone or together with L1 did not result in any significant increase in cofilin-1 phosphorylation in HEK cells (Fig. 4A,B). However, silencing of Gα$_{13}$ led to a significant BIMU8-mediated increase in cofilin-1 phosphorylation only in cells co-expressing 5-HT$_4$R and L1, and not in cells expressing 5-HT$_4$R or L1 alone (Fig. 4). This result suggests that the 5-HT$_4$R–L1 interaction co-activates an additional signaling pathway that inhibits cofilin-1 phosphorylation via Gα$_{13}$.

5-HT$_4$R interacts with L1 in the mouse brain

Next, we investigated whether the endogenous 5-HT$_4$R and L1 interact in the mouse brain by immunolabeling with specific antibodies against 5-HT$_4$R and L1. Microscopic analysis revealed tight colocalization of the 5-HT$_4$R and L1 immunolabeling in the hippocampal CA3 subfield, primary somatosensory, secondary visual and secondary auditory cortex (Fig. 5A). Direct evidence of an interaction between the 5-HT$_4$R and L1 was provided in co-IP experiments in the cortex and hippocampus. Fig. 5B shows that, after immunoprecipitation with an antibody against L1, 5-HT$_4$R was identified in both cortex and hippocampal lysates, suggesting a physical interaction between 5-HT$_4$R and L1 *in vivo*.

The 5-HT$_4$R–L1 module mediates spine maturation but not synaptogenesis in hippocampal neurons

The formation of primary dendrites and dendrite branching are both promoted by activation of the 5-HT$_4$R in developing rat hippocampal neurons *in vitro* (Kozono et al., 2017). We recently demonstrated that the 5-HT$_4$R is involved in functional maturation of dendritic spines (Schill et al., 2020). To elucidate the role of the 5-HT$_4$R–L1 complex in spine formation and synaptogenesis, we used primary cultures of hippocampal neurons, which allowed visualization of the morphological changes. We investigated neurons after 12 days *in vitro* (DIV12), when well-defined synapses are already formed (Bartrup et al., 1997; Kobe et al., 2012). We observed the membrane distribution of the 5-HT$_4$R and L1 as well as their colocalization at the cell soma and synapses, as identified by the presynaptic marker synaptophysin (De Paola et al., 2003) (Fig. 6A).

In line with our recent data (Schill et al., 2020), 5-HT$_4$R activation with BIMU8 significantly increased the number of mushroom spines in neurons transfected with scrambled shRNA (Fig. 6B,C). After selective knockdown of L1 using shRNA, we observed a BIMU8-mediated increase in the number of mushroom spines. However, this increase was significantly diminished

Journal of Cell Science (2021) 134, jcs249193. doi:10.1242/jcs.249193

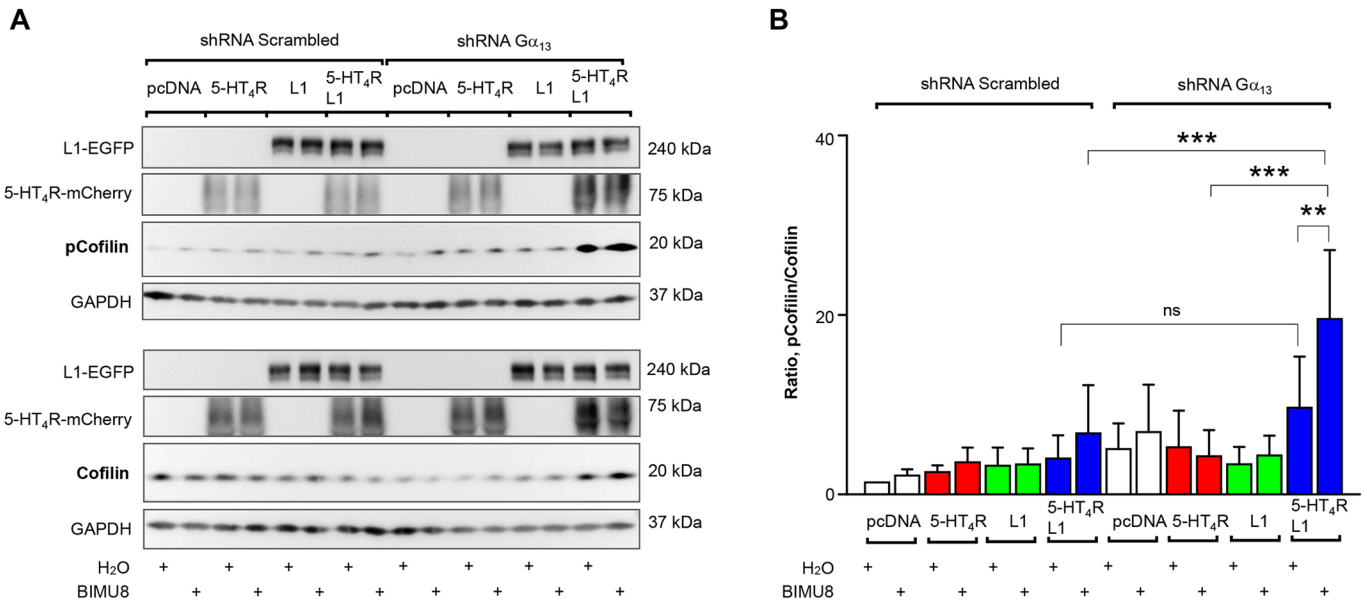

Fig. 4. Interaction between the 5-HT$_4$R and L1 increases cofilin-1 phosphorylation after silencing of Gα_{13}. (A) HEK cells transfected with control vector (pcDNA), 5-HT$_4$R–mCherry (5-HT$_4$R), L1–eGFP (L1), or both 5-HT$_4$R–mCherry and L1–eGFP (5-HT$_4$R/L1) were treated with BIMU8 (5-HT$_4$R agonist) or with water as a vehicle control, and lysates were blotted for the indicated proteins. GAPDH is shown as a loading control. In HEK cells co-transfected with 5-HT$_4$R and L1, treatment with BIMU8 resulted in increased cofilin-1 phosphorylation (pCofilin) after silencing of Gα_{13} (shRNA Gα_{13}). Non-targeting shRNA was used as a control (shRNA scrambled). (B) Quantitative analysis of pCofilin:cofilin ratio in western blotting experiments. Data are presented as mean±s.e.m. (n=3). **P<0.01; ***P<0.001; ns, not significant (two-way ANOVA with Tukey's post hoc test).

compared to the increase observed in the BIMU8-treated neurons transfected with scrambled shRNA (Fig. 6B,C). These effects were L1-specific, because they were completely rescued by transfection of neurons with the shRNA-resistant L1–eGFP (Fig. S5). Notably, the overall spine density was not affected by stimulation of the 5-HT$_4$R with BIMU8 in neuronal cultures transfected with scrambled shRNA (Fig. 6B,C), which is in agreement with our recent study (Schill et al., 2020). Taken together, our data suggest that the 5-HT$_4$R–L1 complex is involved in spine maturation.

To determine whether the 5-HT$_4$R–L1 complex affects synaptic density, we quantified the number of synapses by labeling scrambled shRNA RFP-transfected neurons or L1 shRNA-mCherry-transfected neurons with synaptophysin. Silencing of L1 caused a significant decrease in the number of synapses in all three sets of experimental treatments compared to the number of synapses in neurons transfected with scrambled shRNA (Fig. 7A,B), but stimulation or inhibition of 5-HT$_4$R had no effect.

DISCUSSION

The 5-HT$_4$R is known to be involved in the regulation of neuronal morphogenesis and synaptic plasticity (Hagena and Manahan-Vaughan, 2017; Kozono et al., 2017). We recently demonstrated that 5-HT$_4$R activation triggers the maturation of dendritic spines in parallel with transient alteration of cell excitability (Schill et al., 2020). Several studies have suggested that the function of the 5-HT$_4$R is dependent on its ability to form homodimers and heterodimers with other 5-HT$_4$R isoforms, as well as with receptors from other families, such as β_2-adrenergic receptor (Berthouze et al., 2005). Here, using a FRET-based approach, co-IP and immunofluorescence microscopy, we identified the adhesion molecule L1 as a new interaction partner of 5-HT$_4$R in the modulation of intracellular signaling influencing spine maturation.

Results of our co-IP experiments in transfected HEK cells suggest that the 5-HT$_4$R can interact with both full-length L1 as well as L1 fragments of 80 kDa. The latter has been previously identified a product of proteolytic cleavage of the L1 within its third fibronectin type III (FN III) domain by the serine proteases trypsin (Sadoul et al., 1988), proprotein convertase PC5a (encoded by *PCSK5*; Kalus et al., 2003) and plasmin (Mechtersheimer et al., 2001; Nayeem et al., 1999). Other proteases, including ADAM10, ADAM17 (Beer et al., 1999; Gutwein et al., 2003; Maretzky et al., 2005; Mechtersheimer et al., 2001) and serine protease neuropsin (encoded by *KLK8*; Matsumoto-Miyai et al., 2003), can cleave L1 at similar position. Similarly to the 80 kDa L1 fragment, the 32 kDa L1 fragment generated by ADAM10 (Gutwein et al., 2003) is also membrane-bound. Its proteolytic processing by γ-secretase generates a soluble intracellular 28 kDa fragment, shown to enter the nucleus and to modulate gene expression (Riedle et al., 2009). As transmembrane fragments of L1 are involved in regulation of multiple neuronal functions, including neuronal outgrowth, guidance, fasciculation, myelination and synaptogenesis (Kalus et al., 2006; Lutz et al., 2014a,b, 2017, 2012; Maretzky et al., 2005), we assume that their interaction with 5-HT$_4$R might represent a mechanism for the fine-tuning of a wide range of L1-mediated functions.

Our co-IP experiments in transfected HEK cells also revealed the appearance of two L1 bands as a full-length L1 (220 kDa) and its membrane-bound fragment (80 kDa). We suppose that the intracellular and/or transmembrane part of L1 would interact with the receptor. Two lines of evidence support this view: (1) it has been shown that the interaction between serotonin 2C (5-HT$_{2C}$) receptor and close homolog of the L1, CHL1, occurs via the third intracellular loop of the receptor and intracellular part of CHL1 (Kleene et al., 2015); (2) we have previously shown that transmembrane domains TM4 and TM5 can form an interaction interface in case of 5-HT$_{1A}$ receptor dimerization (Gorinski et al., 2012). We assume that the 5-HT$_4$R interacts with the cytosolic L1 terminus in a homologous manner.

Journal of Cell Science (2021) 134, jcs249193. doi:10.1242/jcs.249193

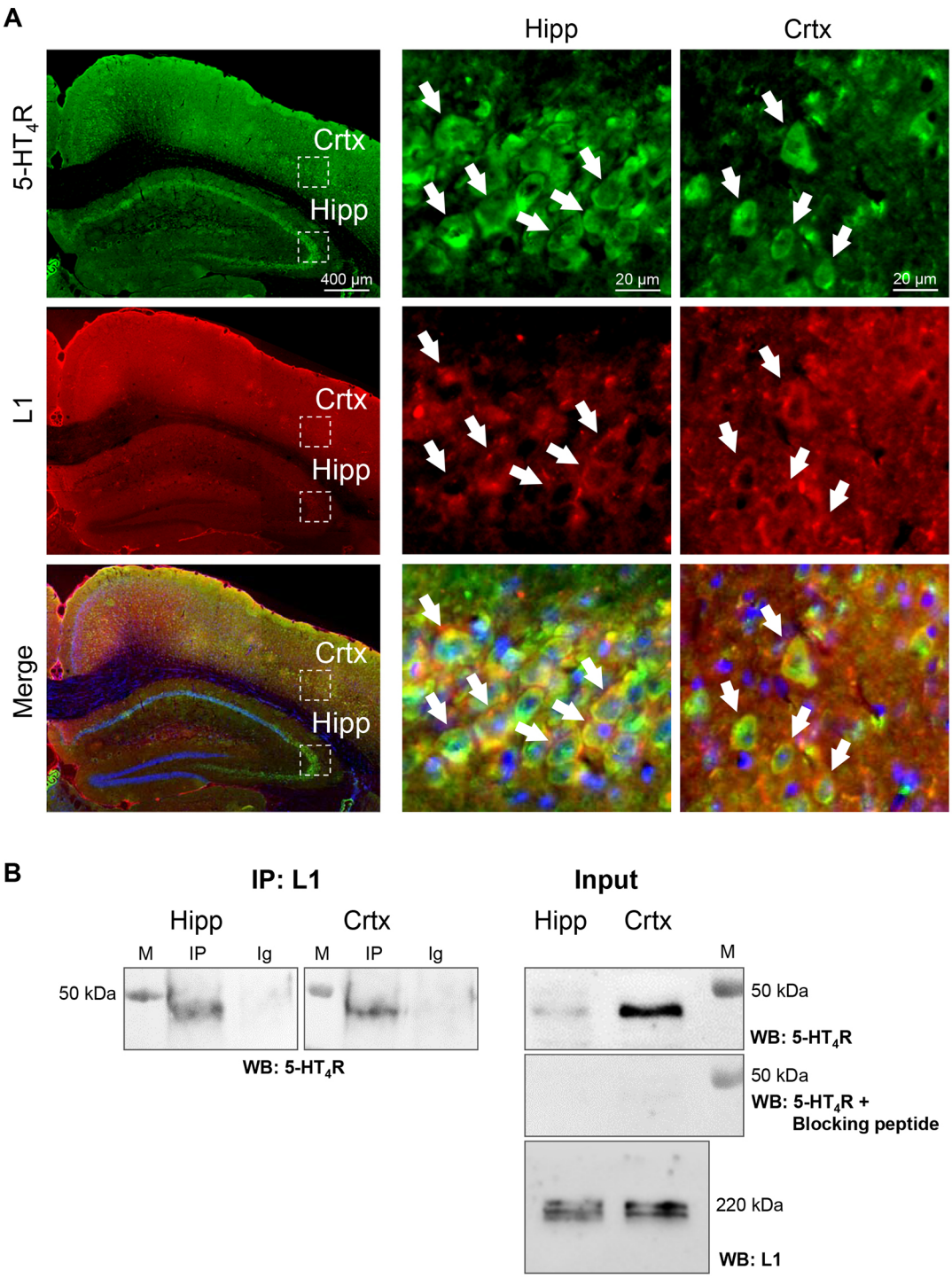

Fig. 5. 5-HT$_4$R and L1 colocalize and interact in the mouse brain. (A) Immunofluorescence analysis of mouse brain sections (left, low magnification; dashed boxes indicate regions shown at high magnification on the right) illustrating the distribution and colocalization (arrows) of the 5-HT$_4$R (green) and L1 (red) in hippocampal (Hipp) and cortical (Crtx) neurons. (B) Co-IP experiments demonstrate the interaction between the 5-HT$_4$R and L1 in the mouse hippocampus (Hipp) and cortex (Crtx) homogenates. Input blots show 25% of total lysate used in co-IP. Addition of a specific blocking peptide demonstrates anti-5-HT$_4$R antibody specificity. M, marker lane; IP, immunoprecipitation; Ig, IgG antibody (negative control); WB, western blot.

In addition to the colocalization of the 5-HT$_4$R and L1 at the plasma membrane of transfected HEK cells, we observed intracellular L1 expression in transfected HEK cells, which is in accordance with previous studies demonstrating that L1 can be localized not only at the cell surface but also in the Golgi complex within the transfected human ovarian carcinoma cell line (Gutwein et al., 2003). Also the 5-HT$_4$R has been shown to reside in the Golgi complex, in addition to its membrane expression, in transfected N1E-115 cells (Niebert et al., 2017). We thus assume that the colocalization of the 5-HT4R and L1 might reflect their heterodimerization during trafficking from the Golgi complex to the cell surface.

Journal of Cell Science (2021) 134, jcs249193. doi:10.1242/jcs.249193

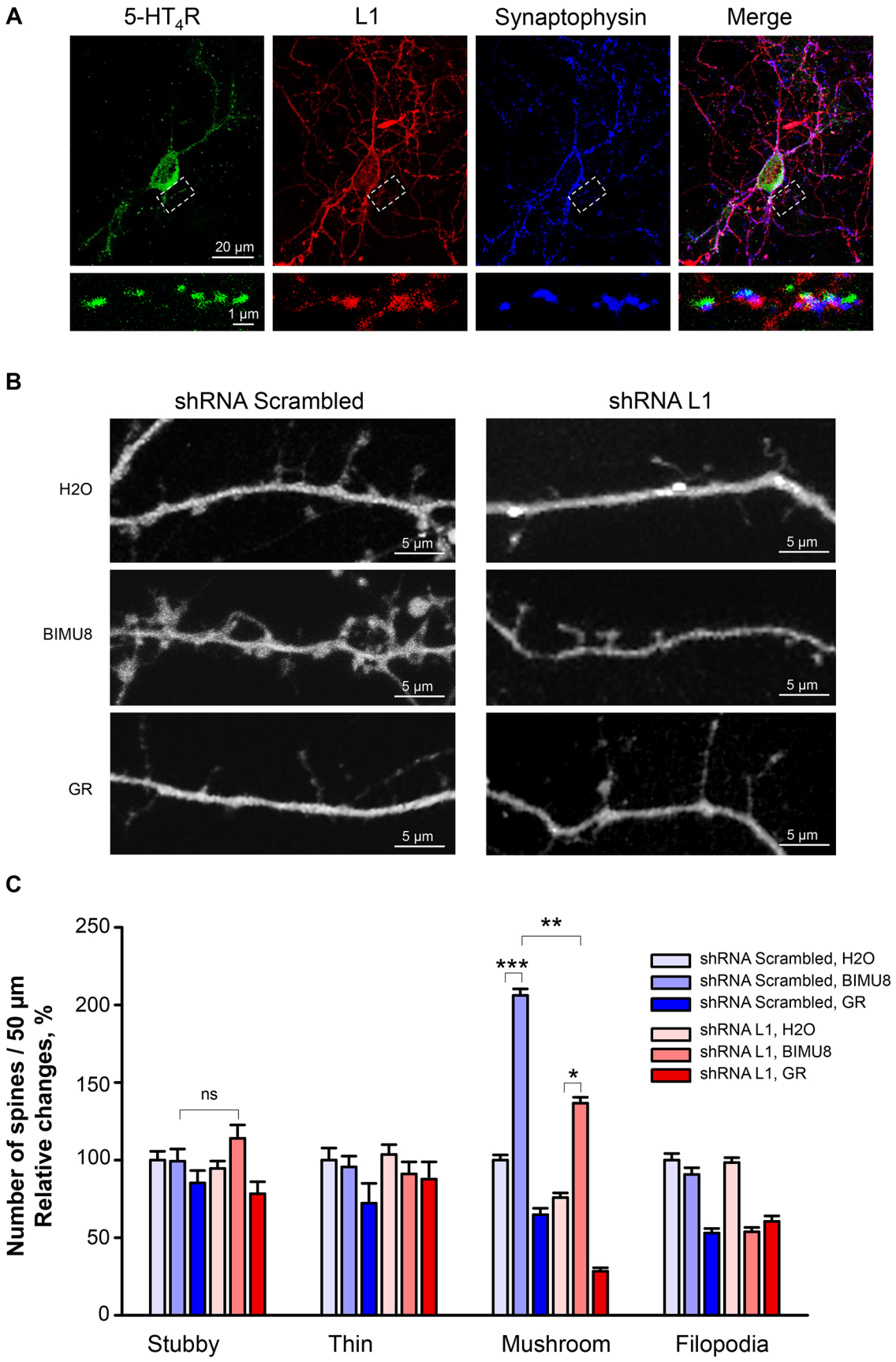

Fig. 6. See next page for legend.

Journal of Cell Science (2021) 134, jcs249193. doi:10.1242/jcs.249193

Fig. 6. 5-HT$_4$R-induced spine formation is L1-dependent. (A) Representative image of a hippocampal neuron at DIV11. Expression of the 5-HT$_4$R was observed in the cell body, dendrites and synapses. Dashed boxes indicate the region shown beneath in high-magnification images that represent a part of the dendrite where the 5-HT$_4$R (green) colocalizes with L1 (red) at the synapse. Blue, synaptophysin. (B) Representative images of dendrites with spines at DIV12 from cells transfected with either shRNA targeting L1 (fluorescence signal shown is mCherry) or control scrambled shRNA (fluorescence signal shown is RFP), and treated with either BIMU8, GR113808 (GR) or water as a vehicle control. (C) Quantification of spines with stubby, thin, mushroom or filopodia morphology for each experimental condition. Data are presented as mean±s.e.m. (n=3 cultures, at least five neurons per condition per experiment). *P<0.05; **P<0.01; ***P<0.001; ns, not significant (ANOVA with Tukey's post hoc test).

We demonstrated that the 5-HT$_4$R–L1 interaction results in a strong facilitation of 5-HT$_4$R-mediated ERK phosphorylation. L1 alone did not have any effect on ERK activation, and requires application of its specific function-triggering antibody to modulate ERK (Schmid et al., 2004, 2000). The 5-HT$_4$R can induce ERK phosphorylation via activation of G$_s$-mediated signaling and/or β-arrestin1–Src-associated ERK activation (Barthet et al., 2009, 2007). The results of our experiments support the Src-dependent scenario. Knocking down the Gα$_s$ subunit in cells expressing 5-HT$_4$R alone did not affect BIMU8-mediated ERK activation, demonstrating that activation of 5-HT$_4$R in HEK cells leads to G$_s$-independent ERK activation. In contrast, silencing the Gα$_s$ subunit in 5-HT$_4$R–L1 co-transfected HEK cells led to a significant reduction in BIMU8-mediated ERK phosphorylation to the levels obtained in cells transfected with scrambled shRNA and expressing 5-HT$_4$R alone. These data suggest that heterodimerization of 5-HT$_4$R and L1 can increase ERK activation through additional recruitment of G$_s$-mediated signaling (Fig. 8).

Our recent study linked 5-HT$_4$R-mediated changes in dendritic spine morphology to the G$_{13}$/RhoA/cofilin signaling pathway (Schill et al., 2020). In the present study, we evaluated the role of 5-HT$_4$R–L1 heterodimerization in regulating this pathway by silencing the Gα$_{13}$ subunit and analyzing receptor-mediated cofilin-1 phosphorylation in HEK cells. Interestingly, we found a significant increase in BIMU8-induced cofilin-1 phosphorylation after knocking down the Gα$_{13}$ subunit in cells co-expressing 5-HT$_4$R and L1. These results suggest that the 5-HT$_4$R–L1 interaction activates an additional signaling pathway leading to cofilin-1 phosphorylation, which is actively inhibited by G$_{13}$ (Fig. 8). One possible mechanism may be related to PAK–LIMK activation, with a subsequent increase in cofilin phosphorylation (Arber et al., 1998; Edwards et al., 1999; Schmid et al., 2004; Yang et al., 1998). Increased cofilin-1 phosphorylation after the ablation of G$_{13}$ can also be explained by possible alterations in the activity of other kinases, such as testicular protein kinase 1 and 2 (TESK1 and TESK2; Toshima et al., 2001a,b), or phosphatases of the slingshot family or the phosphatase chronophin (encoded by *PDXP*), which are known to dephosphorylate cofilin at Ser3 (Gohla et al., 2005; Niwa et al., 2002).

One important consequence of 5-HT$_4$R stimulation is maturation and stabilization of dendritic spines via G$_{13}$-dependent activation of RhoA (Schill et al., 2020). Here, we demonstrated that L1 strongly facilitates these receptor-mediated effects. One possible mechanism of 5-HT$_4$R–L1-mediated spine maturation may be related to the increased ERK phosphorylation observed in our *in vitro* experiments with HEK cells. PKC- and ERK-mediated mushroom spine formation, which is associated with a long-term increase in network activity and functional synaptic connectivity, has been demonstrated in dissociated rat hippocampal cell culture (Goldin and Segal, 2003). Alternatively, the coupling of 5-HT$_4$R to L1 can modulate multiple spatiotemporal Rho GTPase signaling networks involved in different morphological processes, including guanine-nucleotide-exchange factors (GEFs), GTPase-activating proteins (GAPs), GTPases and effectors. GEF proteins play a pivotal role in the activation of small GTPases by promoting GDP–GTP exchange (Schmidt and Hall, 2002). L1 has been shown to promote tyrosine phosphorylation of Vav2 protein, one of the well-established GEFs for Rac1 and Cdc42 (Abe et al., 2000), increasing its GEF activity toward Rac1 (Moon and Gomez, 2010). The 5-HT$_4$R has also been shown to activate Rac (Maillet et al., 2003), suggesting Rac as a possible partner in the 5-HT$_4$R–L1-mediated intracellular signaling pathway. On the other hand, in the brain, small GTPases may function in a hierarchical cascade in which L1-mediated Rac1 activation activates RhoA (Li et al., 2002), further facilitating the 5-HT$_4$R–RhoA signaling leading to spine maturation.

In addition, RhoA activation can be regulated by Gα$_q$ (Chikumi et al., 2002; Swenson-Fields et al., 2008), a pathway necessary for regulation of microtubule dynamics and neuronal growth (Nordman and Kabbani, 2014). As 5-HT$_4$R-mediated cofilin phosphorylation and its downstream effects are mediated solely by the Gα$_{13}$ protein (Schill et al., 2020), we can suppose that L1 interacts directly with Gα$_q$ to induce RhoA-mediated cofilin-1 phosphorylation, or interacts with Gα$_q$-coupled receptors, such as 5-HT$_2$R (Cussac et al., 2002). Functional heterodimerization of the 5-HT$_{2C}$R (encoded by *HTR2C*) with the cell adhesion molecule close homolog of L1 (CHL1) has been demonstrated *in vivo*, suggesting that some functions of these molecules are related to their molecular association (Kleene et al., 2015). The mechanisms by which L1 modulates cofilin-1 phosphorylation in association with serotonergic signaling have to be elucidated. Our data are in accordance with previous studies indicating that deficiency of L1 causes pronounced defects in synaptic formation and plasticity (Enneking et al., 2013; Kudumala et al., 2013; Luthi et al., 1994). The evidence of 5-HT$_4$R–L1-associated morphogenesis is also in line with a previous study indicating that the morphogenic effect of a homolog of vertebrate L1 (SAX-7) requires its co-ligand MeNoRin (dendritic branching protein, MNR-1) to exert its instructive function in developing neuronal dendrites in the model nematode *Caenorhabditis elegans* (Dong et al., 2013; Salzberg et al., 2013). In conclusion, we have demonstrated that the modulatory effect of the 5-HT$_4$R on spine formation and maturation is dependent on its interaction with cell adhesion molecule L1. Thus, we have revealed a new mechanism by which serotonin can function as a modulator of neuronal morphology via 5-HT$_4$R–L1-mediated signal transduction, which represents a potential target for the treatment of neurological and neurodegenerative diseases associated with changes in spine plasticity.

MATERIALS AND METHODS

Animals

Adult (8-to-12-week old) male and female C57BL/6J mice were used for the co-IP and immunofluorescence analyses. C57BL/6J pups were used on postnatal day 0 (P0) for the preparation of dissociated hippocampal cell cultures. Mice were bred and housed at the animal facility of Hannover Medical School under controlled temperature (25°C) and photoperiod (12 h/12 h light/dark cycle), and allowed unrestricted access to standard food and tap water. This study was conducted in accordance with the German law for animal protection and with European Communities Council Directive 86/609/EEC for the protection of animals used for experimental purposes. All experiments were approved by the Local Institutional Animal Care and Research Advisory committee and permitted by the local government (84-02.04.2012.A212, 2017/150, 2018/179).

Journal of Cell Science (2021) 134, jcs249193. doi:10.1242/jcs.249193

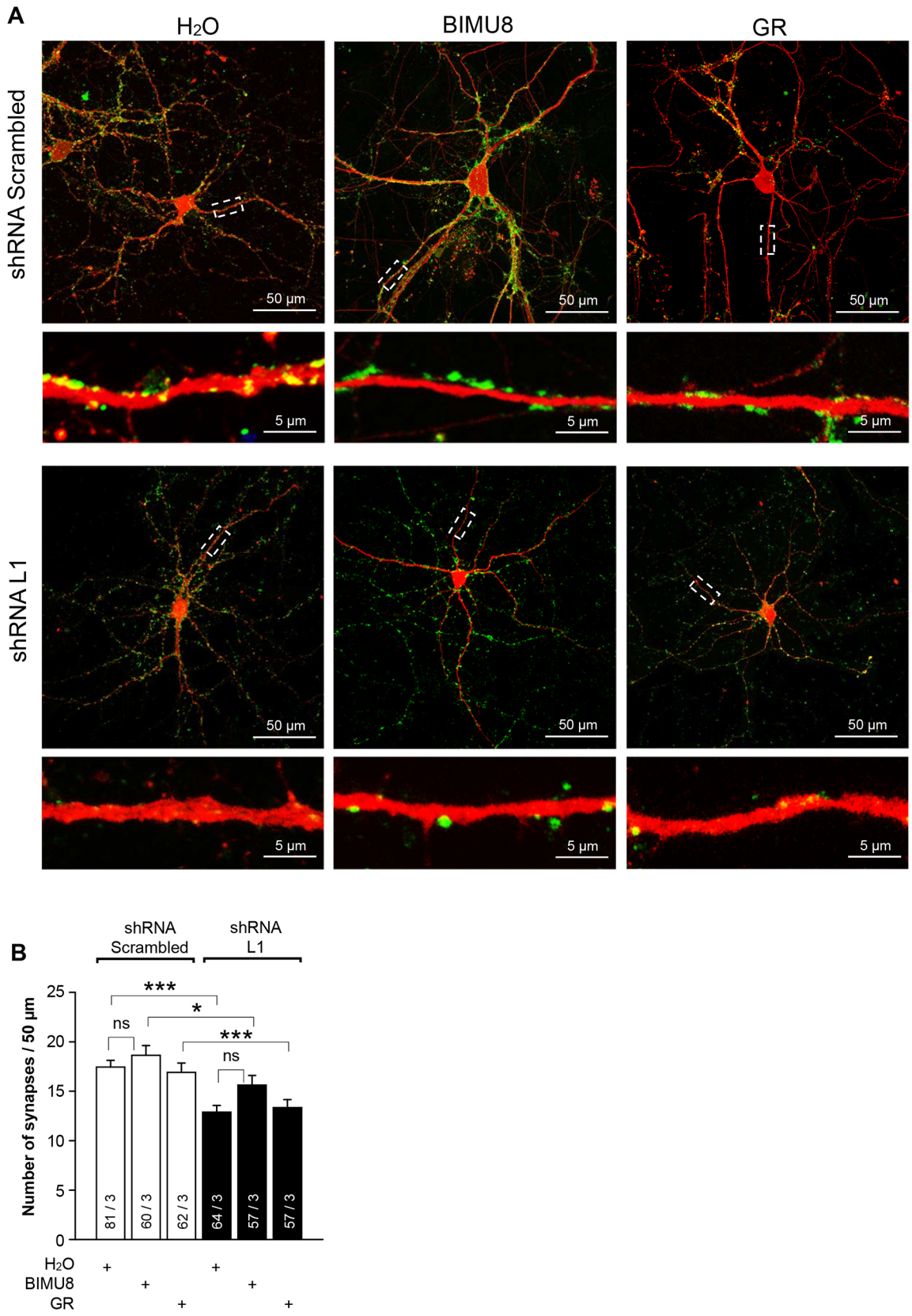

Fig. 7. L1-mediated synaptogenesis is 5-HT$_4$R independent. (A) Representative images of hippocampal neurons at DIV12 and synapses. Cells were transfected with constructs for expression of either shRNA targeting L1 (fluorescence signal shown is mCherry) or control scrambled shRNA (fluorescence signal shown is RFP), and were treated with either BIMU8, GR113808 (GR) or water as a vehicle control. Green, synaptophysin. Dashed boxes indicate regions shown at higher magnification beneath. (B) Quantification of synaptophysin-positive puncta. Data are presented as mean±s.e.m. The *n* is indicated in the bars and represents the total number of dendritic segments/total number of independent cultures. **P*<0.05; ****P*<0.001; ns, not significant (two-way ANOVA with Tukey's post hoc test).

Journal of Cell Science (2021) 134, jcs249193. doi:10.1242/jcs.249193

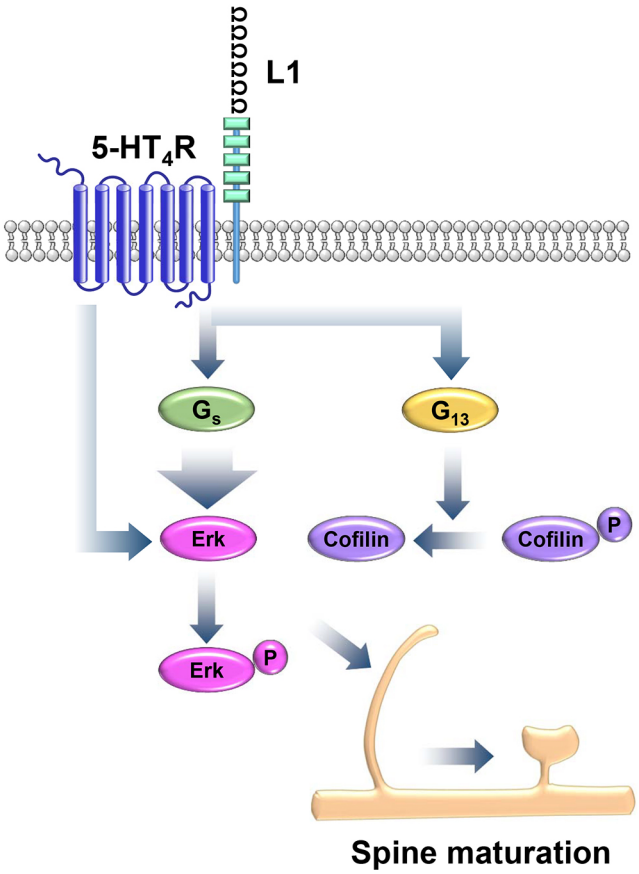

Fig. 8. Schematic representation of intracellular signaling mediated by the 5-HT$_4$R–L1 complex. The interaction between 5-HT$_4$R and L1 facilitates ERK activation and modulates cofilin-1 activity, thereby regulating receptor-dependent maturation of dendritic spines.

Recombinant DNA procedures, shRNA constructs, AAV vectors

The expression plasmids used in this study are listed in Table S1. The double-stranded shRNA sequences were used to target human Gα_s (5′-gattgaggactactttcca-3′), human Gα_{13} (5′-gatgatgtcgtttgatacc-3′), and mouse L1 (5′-tgtaaatacaccgtgactt-3′). One small RNA duplex that has no silencing effect was used as a control (5′-actaccgttgttataggtg-3′). These sequences were designed as double-stranded shRNAs according to available protocols (https://www.invivogen.com/review-sirna-shrna-design), were flanked with BglII (5′ end) and SalI (3′ end) restriction enzyme recognition sites, and were chemically synthesized and cloned into a pAAV-Syn(0.5)-RFP-H1-2 vector plasmid (Cell Biolabs Inc., San Diego, USA) under control of the H1-2 promoter. After cloning, the shRNAs were sequenced, verified, described and validated (Fig. S2). Mouse-specific shRNA against L1 was subcloned into the pAAV-Syn(0.5)-mCherry-H1-2 vector (Cell Biolabs Inc.) at the BglII and SalI restriction sites. Similarly, scrambled shRNA was subcloned for use as a control. The resulting plasmids were co-transfected with DJ vector and pHelper (Cell Biolabs, San Diego, CA) in HEK293 cells (ATCC, Manassas, USA) using polyethylenimine (PEI, Polysciences, 23966-2, Warrington, PA). AAVs were collected after 48 h according to a protocol described previously (Grimm et al., 2003), and then used for experiments *in vitro* with dissociated hippocampal neurons at a final concentration of 10^7 viral particles/µl.

HEK cell culture and transfection

HEK293 cells were cultured in DMEM (Sigma-Aldrich, D5648, Darmstadt, Germany) supplemented with 10% fetal bovine serum (FBS Superior, Biochrom, S0615, Berlin, Germany) and 1% penicillin-streptomycin (5000 U/ml, 15070-063, Thermo Fisher Scientific, Waltham, MA) at 37°C in an incubator humidified with 95% air and 5% CO_2. For western blotting, cells were cultured in 35-mm dishes. For microscopic analysis, cells were cultured on 18-mm glass coverslips placed in 12-well culture plates. Transient transfection was performed with Lipofectamine 2000 (Thermo Fisher Scientific, 11668019) according to the manufacturer's instructions.

Lux-FRET analysis in living HEK cells

To study the interaction between 5-HT$_4$R and L1, FRET analysis was performed in living HEK cells. Cells were grown on 18-mm coverslips for 24 h and co-transfected with plasmids encoding mTurquoise2 (mTq2)-tagged 5-HT$_4$R (5-HT$_4$R–mTq2, donor) and YPet-tagged L1 (L1–YPet, acceptor) (Table S1). As a negative control, we used constructs encoding mTq2-tagged CD86 (CD86–mTq2) and YPet-tagged CD86 (CD86–YPet) (Table S1); CD86 is a monomer and represents an appropriate negative control in studies analyzing protein–protein interactions by resonance energy transfer (Bijata et al., 2017; Dorsch et al., 2009; James et al., 2006; Renner et al., 2012). Twenty-four hours after transfection, cells were imaged using a Zeiss LSM 780 confocal laser scanning microscope (Jena, Germany) equipped with an C-Apochromat 40×/1.2 water immersion objective in Tyrode buffer (pH 7.4; 150 mM NaCl, 5 mM KCl, 1 mM $MgCl_2$, 2 mM $CaCl_2$, 10 mM HEPES; all from Carl Roth, Karlsruhe, Germany) by exciting the fluorescent proteins at 440 and 514 nm according to a previously established protocol (Prasad et al., 2013). To determine the apparent FRET efficiencies (Ef_D and Ef_A) between donor and acceptor, and the donor mole fraction (x_D), the lux-FRET method was used (Zeug et al., 2012). The predicted apparent FRET efficiency was introduced as Ef_{DA} at x_D=0.5, which allows a comparison between different experiments with varying x_D. The Ef_{DA} was calculated assuming a standard dimerization model (Meyer et al., 2006): $Ef_{DA}=½Ef_D(1-x_D)$. Reference spectra were obtained from singly transfected cells expressing either 5-HT$_4$R–mTq2 or L1–YPet, and reference values for the FRET efficiency of the donor and acceptor were calculated from images of HEK cells transfected with a tandem construct consisting of the two fluorophores coupled to each other by a short linker, mTq2–84–Ypet (Table S1). The data from the FRET-based experiments were analyzed using MATLAB scripts.

Co-immunoprecipitation in transfected HEK cells and western blotting

Co-IP with HEK cells co-expressing hemagglutinin (HA)-tagged 5-HT$_4$R (5-HT$_4$R–HA; Table S1) and eGFP-tagged L1 (L1–eGFP; Table S1) was performed 24 h after transfection, as described previously (Kobe et al., 2008). Briefly, cells were washed in phosphate-buffered saline (PBS) and lysed in 1 ml RIPA buffer 1 [150 mM NaCl, 20 mM Tris-HCl pH 7.4, 1% Triton X-100, 1% deoxycholic acid sodium salt, 10 mM EDTA, 10 mM iodoacetamide, 1 mM PMSF, 1 mM CLAP (all from Carl Roth) and 0.1% SDS (Serva)] for 30 min on ice. Lysates were centrifuged at 18,400 ***g*** for 10 min at 4°C. The 5-HT$_4$R–HA or L1–eGFP proteins were immunoprecipitated from the supernatant by incubation with mouse anti-HA antibody (F-7, 1:50, sc-7392, Santa Cruz Biotechnology, Dallas, Texas) or rabbit anti-GFP antibody (1:200, Sigma-Aldrich, AB3080), respectively, overnight at 4°C. Afterwards, lysates were incubated with protein A-sepharose (Sigma-Aldrich, P-3391) for 2 h at 4°C. The immunoprecipitate–sepharose complexes were washed with RIPA buffer 1, eluted with 50 µl Thorner buffer [8 M urea (Serva), 5% SDS, 40 mM Tris-HCl pH 6.8, 0.1 mM EDTA and 0.4 mg/ml Bromophenol Blue (all from Carl Roth)], and centrifuged at 16,400 ***g*** for 10 min at room temperature. Next, 23 µl of each sample was separated by 10% SDS–PAGE and subjected to western blotting. After incubation with goat anti-GFP horseradish peroxidase (HRP)-coupled (1:1000, LS-C50850, LifeSpan BioSciences, Seattle, WA) or rat anti-HA HRP-coupled antibody (1:500, 12013819001, Roche, Basel, Switzerland), both diluted in 5% non-fat dry milk in Tris-buffered saline (TBS) supplemented with 0.1% Tween 20 (TBS-T), proteins were visualized with SuperSignal West Femto Maximum Sensitivity substrate (Thermo Fisher Scientific, 34095) using a Fusion SL Vilber Lourmat System (Peqlab Biotechnologies GmbH, France).

Co-immunoprecipitation in mouse brain lysates and western blotting

Co-IP was performed with the hippocampi and prefrontal cortexes of 3-month-old C57BL/6J mice as described previously (Renner et al., 2012).

Journal of Cell Science (2021) 134, jcs249193. doi:10.1242/jcs.249193

The mouse brain tissue was homogenized in homogenization buffer (pH 7.4, 10 mM HEPES, 5 mM EGTA, 1 mM EDTA, 320 mM sucrose, 1 mM PMSF and 1 mM CLAP) as 100 mg tissue/1 ml buffer. Membrane fractions were prepared by three steps of centrifugation at 4°C: (1) 300 ***g*** (10 min), (2) the supernatants from step 1 at 800 ***g*** (10 min), (3) the supernatants from step 2 at 20,817 ***g*** (1 h). The pellets were resuspended in 500 µl lysis buffer (150 mM NaCl, 50 mM Tris-HCl pH 7.4, 5 mM EDTA, 1 mM CLAP, 1 mM PMSF) supplemented with 0.2% Triton X-100, and incubated at 4°C for 1 h with end-to-end rotation before centrifugation at 20,817 ***g*** (1 min). The anti-L1 antibody (Covance, MMS-172R-500), used in our study for the immunofluorescence analysis of L1 distribution in cultured hippocampal neurons and brain cryoslices, has previously been reported to recognize L1 on western blots of whole brain extracts and to immunoprecipitate mammalian and chick L1 (Lemmon et al., 1989). However, this antibody has a limitation, because it recognizes a dephosphorylated YRSL motif (amino acids 1179–1182 of mouse L1) in the cytoplasmic part of L1 (Schaefer et al., 2002). Since a dephosphorylation of L1 at this site induces its internalization and may also affect interaction with 5-HT_4R, in our co-IP experiments with mouse brain lysates we used the mouse monoclonal anti-L1 antibody (ab24345, Abcam, Cambridge, UK) that is directed against the conserved whole cytoplasmic domain of L1 (human and mouse L1 amino acids 1144–1257). The supernatants (100 µl) were incubated with the mouse antibody against L1 (1:100, ab24345, Abcam, Cambridge, UK) in 500 µl of lysis buffer at 4°C overnight with end-over-end rotation. Mouse IgG antibody (1:100, Sigma-Aldrich, I5381) was used as a negative control. Immunoprecipitation was performed with 80 µl of Protein G Sepharose 4 Fast Flow (GE Healthcare, 17-0618-01) suspension at 4°C with end-over-end rotation for 2 h, followed by centrifugation at 4°C for 1 min at 6000 ***g***. The pellets were washed five times with lysis buffer by centrifugation, incubated at 37°C for 20 min with 50 µl Thorner buffer, centrifuged again at room temperature at 16,400 ***g*** for 3 min, and separated by 10% SDS–PAGE. After western blotting, the membranes were incubated with 5% non-fat dry milk in TBS-T and then with a rabbit antibody against 5-HT_4R (1:500, ASR-036, Alomone, Jerusalem, Israel) diluted in 5% non-fat dry milk in TBS-T. The specificity of the anti-5-HT_4R antibody was verified using pre-incubation with a specific blocking peptide (5-HT_4R ext. 168–180 Peptide, Alomone, 1:1 in PBS, 2 h at room temperature; Fig. 5B). Visualization was achieved using the secondary goat anti-rabbit HRP-coupled antibody (1:10,000, Thermo Fisher Scientific, 31460) and the system described above.

Drugs and treatment

Transfected HEK cells were treated with the 5-HT_4R agonist BIMU8 (10 µM, 4374, Tocris, Bristol, UK) or the specific 5-HT_4R antagonist GR113808 (GR; 10 µM, 1322, Tocris) for 5 min at 37°C in a 5% CO_2 humidified atmosphere. The simultaneous application of both was used to confirm the specificity of the agonist. Cells were first incubated with GR113808 for 30 min, then BIMU8 was applied and the cells incubated for another 5 min. Water was used as a control. Directly after incubation, the cells were lysed.

For the treatment of dissociated hippocampal neurons, the following concentrations of agonist and antagonist were used: 100 nM BIMU8 and 100 nM GR113808. Drugs were added to cultures starting from *in vitro* day 7 (DIV7) and each following day until DIV14. Water was used as a control. On DIV14, cells were fixed and subjected to immunofluorescence analysis.

ERK and cofilin phosphorylation assays in transfected HEK cells

To determine the significance of the 5-HT_4R–L1 interaction for ERK and cofilin phosphorylation, HEK cells co-transfected with 5-HT_4R–mCherry and L1–eGFP were treated as described above. Directly after treatment, cells were washed once with PBS and lysed in RIPA buffer 2 (137 mM NaCl, 20 mM Tris-HCl pH 7.5, 25 mM β-glycerophosphate, 1 mM sodium orthovanadate, 1% Triton X-100, 50 mM sodium fluoride, 1% deoxycholic acid sodium salt, 2 mM EDTA, 1 mM PMSF and 1 mM CLAP). After collection and centrifugation, the supernatants were heated with loading buffer supplemented with 5% β-mercaptoethanol at 56°C for 10 min, separated by 12% SDS–PAGE and subjected to western blotting. Non-specific binding was blocked with 5% BSA in TBS-T. The following primary antibodies were applied overnight at 4°C: rabbit anti-Erk1/2 (1:2000, 9102, Cell Signaling, Danvers, MA) or rabbit anti-pErk1/2 (1:2000, 9101, Cell Signaling), both diluted in 5% BSA in TBS-T; mouse anti-GAPDH (1:10,000, GTX 627408, Gene Tex, Irvine, CA) or goat anti-mCherry (1:1000, AB0040-200, SICGEN Antibodies, Cantanhede, Portugal), both diluted in 5% non-fat milk in TBS-T.

To analyze the role of $G\alpha_s$ protein in ERK phosphorylation induced by the interaction between 5-HT_4R and L1, we used shRNA against the human $G\alpha_s$ subunit and scrambled shRNA as a control (Table S1). HEK cells were co-transfected with 5-HT_4R–mCherry, L1–eGFP and shRNA, and analyzed as described above. To analyze the role of the $G\alpha_{13}$ subunit in cofilin phosphorylation induced by the interaction between 5-HT_4R and L1, we used shRNA against human $G\alpha_{13}$ and scrambled shRNA as a control (Table S1). Here, cofilin phosphorylation was identified using the following antibodies: rabbit anti-Cofilin-1 (1:4000, Cell Signaling, 5175S) or rabbit anti-pCofilin (1:4000, Cell Signaling, 3311S), both diluted in 5% BSA in TBS-T. Visualization was performed with the appropriate secondary goat anti-rabbit (1:10,000, Thermo Fisher Scientific, 31460), rabbit anti-mouse (1:10,000, Thermo Fisher Scientific, 31455), or rabbit anti-goat (1:10,000, Thermo Fisher Scientific, 31402) HRP-coupled antibodies diluted in 5% non-fat milk in TBS-T using the system described above. During the quantification analysis, we first normalized ERK and cofilin-1 protein expression to GAPDH levels detected in the same blot. The same strategy was applied to the pERK and pCofilin. The values, obtained after initial normalization were then used to calculate ERK:pERK and Cofilin:pCofilin ratios.

Culturing, AAV infection and transfection of hippocampal neurons

Mouse primary hippocampal neurons were prepared according to an optimized protocol for mouse hippocampal neurons (Guzman et al., 2010). Brains were isolated from C57BL/6J mice of both sexes on P0 to P3 under sterile conditions and placed in HBSS (Thermo Fisher Scientific, 24020). Hippocampi were dissected from the brain under a stereomicroscope (Leica S6 D Stereozoom 0.63×–4.0×; Wetzlar, Germany) and enzymatically dissociated by incubation for 20 min at 37°C in DMEM (Thermo Fisher Scientific, 31966-021) containing 10 U/ml papain (Worthington, 3126, Lakewood, NJ), 50 mM EDTA, 100 mM $CaCl_2$, and 2 mg/ml cysteine (Sigma-Aldrich, C-7352). After incubation, enzyme dissociation was blocked by incubation for 5 min at room temperature with 10% FBS medium (10% FBS, 0.2% penicillin-streptomycin in DMEM) supplemented with 25 mg/ml albumin (Sigma-Aldrich, A-4503) and 25 mg/ml trypsin inhibitor (Sigma-Aldrich, T-9253). The cells were then gently mechanically resuspended in 10% FBS medium and plated onto 18-mm coverslips coated with 0.2 mg/ml Poly-D-lysine hydrobromide (Sigma-Aldrich, P6407) in 0.1 M borate buffer (pH 8.5). Cultures were maintained at 37°C in an incubator humidified with 95% air and 5% CO_2 in Neurobasal A medium (Thermo Fisher Scientific, 10888-022) supplemented with 2% B-27 Supplement (Thermo Fisher Scientific, 17504-044), 1% GlutaMAX (Thermo Fisher Scientific, 35050-061), 0.2% penicillin-streptomycin, and 0.1% MITO (BD, 355006, Bedford, MA). Neurons were infected on DIV2 with 1 µl AAV per well, which contained constructs expressing either scrambled shRNA and RFP (pAAV_H1_shRNA-Scramble_RFP), or L1 shRNA and mCherry (pAAV_H1_shRNA-mouse_L1_mCherry). Half of the medium was changed on DIV2 and again subsequently every 5th day. Transient transfection in rescue experiments was performed with L1–eGFP or pmax–GFP (Table S1) on DIV7 using Lipofectamine 2000 (Thermo Fisher Scientific), according to the manufacturer's instructions, for 1 h. Morphological analysis (number of stubby, thin, mushroom and filopodia spines; number of synapses) was performed on DIV12 of culture when functional synapses are formed (Kobe et al., 2012).

Immunofluorescence in dissociated hippocampal cell culture and quantification analysis of synapses

To analyze 5-HT_4R and L1 distribution in dissociated hippocampal neurons, cultured cells were fixed with 4% paraformaldehyde (PFA) for 10 min at room temperature on DIV12 and permeabilized with pre-cooled methanol (−20°C) for 3 min. After blocking non-specific binding sites with 3% BSA (Carl Roth) diluted in PBS for 30 min at room temperature, primary antibodies rabbit polyclonal anti-5-HT_4R (1:100, C12017, Assay Biotechnology, Sunnyvale, CA), mouse monoclonal anti-L1 (1:200,

Covance, MMS-172R-500) and goat polyclonal anti-synaptophysin (1:50, Santa Cruz Biotechnology, sc-7392) diluted in PBS containing 3% BSA were applied overnight at 4°C. After washing with PBS, appropriate secondary antibodies were applied at room temperature for 30 min: donkey anti-rabbit DyLight 405-conjugated (Jackson ImmunoResearch, 711-475-152), donkey anti-mouse DyLight 649-conjugated (Jackson ImmunoResearch, 715-495-151) and donkey anti-goat Alexa Fluor 488-conjugated (Jackson ImmunoResearch, 705-545-147) antibodies diluted 1:400 in PBS containing 3% BSA. After subsequent washing with PBS, the coverslips were mounted in Fluoromount G anti-quenching medium and subjected to imaging analysis using a confocal microscope (Zeiss LSM 780) with a 40× or 63× oil-immersion objective. To analyze the number of synaptic clusters, synaptophysin-positive puncta were calculated along the dendrites of neurons infected with AAV encoding either shRNA against L1 or scrambled shRNA. At least five neurons (50 dendritic segments) from three independent cultures were used for each treatment protocol. Proximal dendritic segments were analyzed from both primary and secondary dendrites at distances between 30–100 µm from the cell body. The number of synaptophysin-positive puncta was calculated per 50 µm of the entire dendritic length. All experiments were performed in a double-blind manner (i.e. investigators were blinded to AAV infection and treatment) to avoid any subjective influences during the measurements.

Western blotting and qPCR in dissociated hippocampal cell culture

To test the efficiency of the shRNA against mouse L1, cultured hippocampal neurons were infected with shRNA L1 or shRNA scrambled on DIV2. On DIV12, cell cultures were washed once with PBS and lysed in MAP-Kinase lysis buffer (150 mM NaCl, 50 mM Tris-HCl pH 7.5, 1 mM sodium orthovanadate, 1% Triton X-100, 0.1% SDS, 50 mM sodium fluoride, 0.5% deoxycholic acid sodium salt, 10 mM disodium dihydrogen pyrophosphate, 1 mM PMSF and 1 mM CLAP). After collection and centrifugation, the supernatants were heated with loading buffer supplemented with 5% β-mercaptoethanol at 95°C for 10 min, separated by 10% SDS–PAGE and subjected to western blotting. Non-specific binding was blocked with 5% non-fat milk in TBS-T. The following primary antibodies were applied overnight at 4°C: mouse anti-L1 (1:1000, Abcam, ab24345) and rabbit anti-βIII-tubulin (1:2000, 802001, BioLegend, San Diego, CA), both diluted in 5% milk in TBS-T. Visualization was performed with rabbit anti-mouse HRP-conjugated (Thermo Fisher Scientific, 31455) or goat anti-rabbit HRP-conjugated (Thermo Fisher Scientific, 31460) antibodies, both diluted 1:5000 in 5% milk in TBS-T.

For the real-time quantitative PCR (qPCR) analysis, the total RNA from cultured hippocampal neurons was isolated with an RNeasy Plus Mini Kit (74136, Qiagen, Hilden, Germany), and cDNA was synthetized using SuperScript III First-Strand (Invitrogen, 18080-051, Waltham, MA). Expression analysis was performed on a StepOnePlus real-time PCR system (Applied Biosystems, Darmstadt, Germany) using TaqMan Universal PCR Master Mix (Applied Biosystems, 4324018, Warrington, UK). For the detection of L1 (*L1cam*) mRNA, gene-specific forward (5′-TGCTCATCCTCTGCTTCATC-3′) and reverse (5′-CCTTCTCTTCATTG-TCACTCTCC-3′) primers and probe (5′-AAGGTCTCGTCTTTCATGGG-CCG-3′ with reporter 6-FAM/TAMRA) were used. As a housekeeping gene we used *Gapdh*, and used gene-specific forward (5′-TGCACCACCAACT-GCTTAGC-3′) and reverse (5′-GGCATGGACTGTGGTCATGAG-3′) primers, and probe (5′-CCCTGGCCAAGGTCATCCATGACAAC-3′ with reporter 6-FAM/TAMRA). Analysis was performed by using ΔΔCt method according to the procedure described at https://www.thermofisher.com/content/dam/LifeTech/global/Forms/PDF/real-time-pcr-handbook.pdf.

Preparation of mouse brain tissue for morphological analysis

Mice were anesthetized using CO_2 and transcardially perfused with 4% formaldehyde in 0.1 M sodium cacodylate buffer (pH 7.3). The brain was removed, post-fixated overnight at 4°C, and then immersed in 15% sucrose solution in 0.1 M cacodylate buffer (pH 7.3) overnight at 4°C, followed by 30% sucrose in 0.1 M cacodylate buffer overnight at 4°C. Afterwards, the tissue was frozen for 2 min in 2-methyl-butane (isopentane; Carl Roth) precooled to −30°C. For sectioning, the brain was attached to a cryostat specimen holder using TissueTek (Sakura Finetek Europe, Zoeterwoude, The Netherlands). Serial sections 20 µm thick were cut on a cryostat (Microm HM 560 M, Thermo Fisher Scientific, Walldorf, Germany) and transferred to SuperFrostPlus glass slides (Thermo Fisher Scientific). The sections were air-dried at least overnight at room temperature and subjected further to immunofluorescence analysis.

Immunofluorescence in the mouse brain

Brain cryosections were washed with PBS, and antigen retrieval was performed by immersion in 0.01 M sodium citrate solution (pH 9.0) and heating to 80°C in a water bath for 30 min. Blocking of non-specific binding sites was performed using PBS containing 5% normal donkey serum (Jackson ImmunoResearch Laboratories, 017-000-121), 0.1% Triton X-100 (Sigma-Aldrich, 93427) and 0.02% sodium azide (Merck, Darmstadt, Germany) for 1 h at room temperature. Incubation with rabbit polyclonal anti-5-HT_4R (1:200; SA9106, Synaptic System, Göttingen, Germany) produced by the company at our request via rabbit immunization with a synthetic peptide that corresponds to the C-terminal sequence of the 5-HT_{4a}R isoform, amino acids His^{364} to Pro^{380} (Manzke et al., 2003), or mouse monoclonal anti-L1 (1:200, Covance, MMS-172R-500) diluted in PBS was carried out for 3 days at 4°C. After washing in PBS, appropriate secondary antibodies were applied for 2 h at room temperature: donkey anti-rabbit Alexa Fluor 488-conjugated (Jackson ImmunoResearch, 711-545-152) and donkey anti-mouse DyLight 549-conjugated (Jackson ImmunoResearch, 715-505-151), both diluted 1:200 in PBS. After subsequent washing in PBS, cell nuclei were visualized with bis-benzimide solution (Hoechst 33258 dye, 5 µg/ml in PBS; Sigma-Aldrich). Finally, the sections were mounted in anti-quenching medium (Fluoromount G, Southern Biotechnology Associates, Biozol, Eching, Germany) and subjected to microscopic analysis using a fluorescence microscope (Zeiss Axiovert 200 M; Göttingen, Germany) with 20× and 40× air objectives.

Statistical analysis

All statistical analyses were performed using GraphPad Prism 7 (La Jolla California USA; https://www.graphpad.com/) with the indicated statistical methods in the figure legends. The data are presented as mean±s.e.m. In FRET experiments, the total number of cells and total number of independent cultures are indicated in the bars, and statistical analysis between two groups was performed with unpaired two-tailed Student's *t*-tests. In western blotting experiments, the intensity of bands was quantified using ImageQuantTL v8.1 (Freiburg, Germany) software, and cell lysates from at least three independent HEK cell cultures were taken for the statistical analysis using two-way ANOVA with Tukey's post hoc test. In dissociated hippocampal neurons, images of at least five neurons (20 dendritic segments) per treatment per AAV infection (plasmid transfection) were performed, and the total number of dendritic segments and total number of independent cultures were indicated in the bars. Morphological data (number of spines and number of synapses) from three independent cultures were compared using two-way ANOVA with Tukey's post hoc test.

Acknowledgements

We thank Gundula Bartzke, PhD, for advice on statistical analysis, and Tania Bunke for the excellent technical assistance.

Competing interests

The authors declare no competing or financial interests.

Author contributions

Conceptualization: S.B.S., E.P., D.G.; Methodology: S.B.S., J.R., C.G., N.G., S.K.S., D.A.G., V.N., A.Z., E.P., D.G.; Software: S.B.S., J.R., C.G., N.G., S.K.S., D.A.G., V.N., A.Z., D.G.; Validation: S.B.S., J.R., C.G., N.G., S.K.S., D.A.G., V.N., A.Z., E.P., D.G.; Formal analysis: S.B.S., J.R., C.G., N.G., S.K.S., D.A.G., V.N., A.Z., D.G.; Investigation: S.B.S., J.R., C.G., N.G., S.K.S., D.A.G., E.P., D.G.; Resources: E.P., D.G.; Data curation: A.Z., E.P., D.G.; Writing - original draft: S.B.S., J.R., C.G., N.G., S.K.S., D.A.G., V.N., A.Z., S.C.B., E.P., D.G.; Writing - review & editing: S.B.S., S.C.B., E.P., D.G.; Visualization: S.B.S., J.R., C.G., N.G., E.P., D.G.; Supervision: E.P., D.G.; Project administration: E.P., D.G.; Funding acquisition: E.P., D.G.

Funding

This work was supported by the German Research Foundation (Deutsche Forschungsgemeinschaft, DFG) through DFG grants GU 1521/4-1 to D.G. and

PO732 to E.P. E.P. was further supported through Lobachevsky University 5-100 academic excellence program. E.P and V.N were supported through the budget project 0259-2021-0015.

Supplementary information

Supplementary information available online at
https://jcs.biologists.org/lookup/doi/10.1242/jcs.249193.supplemental

Peer review history

The peer review history is available online at
https://jcs.biologists.org/lookup/doi/10.1242/jcs.249193.reviewer-comments.pdf

References

Abe, K., Rossman, K. L., Liu, B., Ritola, K. D., Chiang, D., Campbell, S. L., Burridge, K. and Der, C. J. (2000). Vav2 is an activator of Cdc42, Rac1, and RhoA. *J. Biol. Chem.* **275**, 10141-10149. doi:10.1074/jbc.275.14.10141

Arber, S., Barbayannis, F. A., Hanser, H., Schneider, C., Stanyon, C. A., Bernard, O. and Caroni, P. (1998). Regulation of actin dynamics through phosphorylation of cofilin by LIM-kinase. *Nature* **393**, 805-809. doi:10.1038/31729

Barthet, G., Framery, B., Gaven, F., Pellissier, L., Reiter, E., Claeysen, S., Bockaert, J. and Dumuis, A. (2007). 5-hydroxytryptamine$_4$ receptor activation of the extracellular signal-regulated kinase pathway depends on Src activation but not on G protein or β-arrestin signaling. *Mol. Biol. Cell* **18**, 1979-1991. doi:10.1091/mbc.e06-12-1080

Barthet, G., Carrat, G., Cassier, E., Barker, B., Gaven, F., Pillot, M., Framery, B., Pellissier, L. P., Augier, J., Kang, D. S. et al. (2009). β-arrestin1 phosphorylation by GRK5 regulates G protein-independent 5-HT4 receptor signalling. *EMBO J.* **28**, 2706-2718. doi:10.1038/emboj.2009.215

Bartrup, J. T., Moorman, J. M. and Newberry, N. R. (1997). BDNF enhances neuronal growth and synaptic activity in hippocampal cell cultures. *Neuroreport* **8**, 3791-3794. doi:10.1097/00001756-199712010-00027

Beer, S., Oleszewski, M., Gutwein, P., Geiger, C. and Altevogt, P. (1999). Metalloproteinase-mediated release of the ectodomain of L1 adhesion molecule. *J. Cell Sci.* **112**, 2667-2675.

Berthouze, M., Ayoub, M., Russo, O., Rivail, L., Sicsic, S., Fischmeister, R., Berque-Bestel, I., Jockers, R. and Lezoualc'h, F. (2005). Constitutive dimerization of human serotonin 5-HT$_4$ receptors in living cells. *FEBS Lett.* **579**, 2973-2980. doi:10.1016/j.febslet.2005.04.040

Bijata, M., Labus, J., Guseva, D., Stawarski, M., Butzlaff, M., Dzwonek, J., Schneeberg, J., Böhm, K., Michaluk, P., Rusakov, D. A. et al. (2017). Synaptic remodeling depends on signaling between serotonin receptors and the extracellular matrix. *Cell Rep.* **19**, 1767-1782. doi:10.1016/j.celrep.2017.05.023

Bockaert, J., Sebben, M. and Dumuis, A. (1990). Pharmacological characterization of 5-hydroxytryptamine4(5-HT4) receptors positively coupled to adenylate cyclase in adult guinea pig hippocampal membranes: effect of substituted benzamide derivatives. *Mol. Pharmacol.* **37**, 408-411.

Chen, J., Wu, J., Apostolova, I., Skup, M., Irintchev, A., Kügler, S. and Schachner, M. (2007). Adeno-associated virus-mediated L1 expression promotes functional recovery after spinal cord injury. *Brain* **130**, 954-969. doi:10.1093/brain/awm049

Chikumi, H., Vázquez-Prado, J., Servitja, J.-M., Miyazaki, H. and Gutkind, J. S. (2002). Potent activation of RhoA by Gαq and Gq-coupled receptors. *J. Biol. Chem.* **277**, 27130-27134. doi:10.1074/jbc.M204715200

Cussac, D., Newman-Tancredi, A., Duqueyroix, D., Pasteau, V. and Millan, M. J. (2002). Differential activation of Gq/11 and Gi$_3$ proteins at 5-hydroxytryptamine$_{2C}$ receptors revealed by antibody capture assays: influence of receptor reserve and relationship to agonist-directed trafficking. *Mol. Pharmacol.* **62**, 578-589. doi:10.1124/mol.62.3.578

De Paola, V., Arber, S. and Caroni, P. (2003). AMPA receptors regulate dynamic equilibrium of presynaptic terminals in mature hippocampal networks. *Nat. Neurosci.* **6**, 491-500. doi:10.1038/nn1046

DeBernardo, A. P. and Chang, S. (1996). Heterophilic interactions of DM-GRASP: GRASP-NgCAM interactions involved in neurite extension. *J. Cell Biol.* **133**, 657-666. doi:10.1083/jcb.133.3.657

Doherty, P. and Walsh, F. S. (1996). CAM-FGF receptor interactions: a model for axonal growth. *Mol. Cell. Neurosci.* **8**, 99-111. doi:10.1006/mcne.1996.0049

Dong, X., Liu, O. W., Howell, A. S. and Shen, K. (2013). An extracellular adhesion molecule complex patterns dendritic branching and morphogenesis. *Cell* **155**, 296-307. doi:10.1016/j.cell.2013.08.059

Dorsch, S., Klotz, K.-N., Engelhardt, S., Lohse, M. J. and Bünemann, M. (2009). Analysis of receptor oligomerization by FRAP microscopy. *Nat. Methods* **6**, 225-230. doi:10.1038/nmeth.1304

Edwards, D. C., Sanders, L. C., Bokoch, G. M. and Gill, G. N. (1999). Activation of LIM-kinase by Pak1 couples Rac/Cdc42 GTPase signalling to actin cytoskeletal dynamics. *Nat. Cell Biol.* **1**, 253-259. doi:10.1038/12963

Eglen, R. M., Wong, E. H. F., Dumuis, A. and Bockaert, J. (1995). Central 5-HT4 receptors. *Trends Pharmacol. Sci.* **16**, 391-398. doi:10.1016/S0165-6147(00)89081-1

Enneking, E.-M., Kudumala, S. R., Moreno, E., Stephan, R., Boerner, J., Godenschwege, T. A. and Pielage, J. (2013). Transsynaptic coordination of synaptic growth, function, and stability by the L1-type CAM Neuroglian. *PLoS Biol.* **11**, e1001537. doi:10.1371/journal.pbio.1001537

Figge, C., Loers, G., Schachner, M. and Tilling, T. (2012). Neurite outgrowth triggered by the cell adhesion molecule L1 requires activation and inactivation of the cytoskeletal protein cofilin. *Mol. Cell. Neurosci.* **49**, 196-204. doi:10.1016/j.mcn.2011.10.002

Frints, S. G. M., Marynen, P., Hartmann, D., Fryns, J.-P., Steyaert, J., Schachner, M., Rolf, B., Craessaerts, K., Snellinx, A., Hollanders, K. et al. (2003). CALL interrupted in a patient with non-specific mental retardation: gene dosage-dependent alteration of murine brain development and behavior. *Hum. Mol. Genet.* **12**, 1463-1474. doi:10.1093/hmg/ddg165

Gibson, N. J. (2011). Cell adhesion molecules in context: CAM function depends on the neighborhood. *Cell Adhes. Migr.* **5**, 48-51. doi:10.4161/cam.5.1.13639

Gohla, A., Birkenfeld, J. and Bokoch, G. M. (2005). Chronophin, a novel HAD-type serine protein phosphatase, regulates cofilin-dependent actin dynamics. *Nat. Cell Biol.* **7**, 21-29. doi:10.1038/ncb1201

Goldin, M. and Segal, M. (2003). Protein kinase C and ERK involvement in dendritic spine plasticity in cultured rodent hippocampal neurons. *Eur. J. Neurosci.* **17**, 2529-2539. doi:10.1046/j.1460-9568.2003.02694.x

Gorinski, N., Kowalsman, N., Renner, U., Wirth, A., Reinartz, M. T., Seifert, R., Zeug, A., Ponimaskin, E. and Niv, M. Y. (2012). Computational and experimental analysis of the transmembrane domain 4/5 dimerization interface of the serotonin 5-HT$_{1A}$ receptor. *Mol. Pharmacol.* **82**, 448-463. doi:10.1124/mol.112.079137

Grimm, D., Kay, M. A. and Kleinschmidt, J. A. (2003). Helper virus-free, optically controllable, and two-plasmid-based production of adeno-associated virus vectors of serotypes 1 to 6. *Mol. Ther.* **7**, 839-850. doi:10.1016/S1525-0016(03)00095-9

Gutwein, P., Mechtersheimer, S., Riedle, S., Stoeck, A., Gast, D., Joumaa, S., Zentgraf, H., Fogel, M. and Altevogt, D. P. (2003). ADAM10-mediated cleavage of L1 adhesion molecule at the cell surface and in released membrane vesicles. *FASEB J.* **17**, 292-294. doi:10.1096/fj.02-0430fje

Guzman, R. E., Schwarz, Y. N., Rettig, J. and Bruns, D. (2010). SNARE force synchronizes synaptic vesicle fusion and controls the kinetics of quantal synaptic transmission. *J. Neurosci.* **30**, 10272-10281. doi:10.1523/JNEUROSCI.1551-10.2010

Hagena, H. and Manahan-Vaughan, D. (2017). The serotonergic 5-HT4 receptor: a unique modulator of hippocampal synaptic information processing and cognition. *Neurobiol. Learn. Mem.* **138**, 145-153. doi:10.1016/j.nlm.2016.06.014

Hall, H., Djonov, V., Ehrbar, M., Hoechli, M. and Hubbell, J. A. (2004). Heterophilic interactions between cell adhesion molecule L1 and $\alpha_v\beta_3$-integrin induce HUVEC process extension in vitro and angiogenesis in vivo. *Angiogenesis* **7**, 213-223. doi:10.1007/s10456-004-1328-5

Heine, M., Ponimaskin, E., Bickmeyer, U. and Richter, D. W. (2002). 5-HT-receptor-induced changes of the intracellular cAMP level monitored by a hyperpolarization-activated cation channel. *Pflugers Arch.* **443**, 418-426. doi:10.1007/s004240100690

Herr, N., Bode, C. and Duerschmied, D. (2017). The effects of serotonin in immune cells. *Front. Cardiovasc. Med.* **4**, 48. doi:10.3389/fcvm.2017.00048

Hortsch, M., Wang, Y.-M. E., Marikar, Y. and Bieber, A. J. (1995). The cytoplasmic domain of the *Drosophila* cell adhesion molecule neuroglian is not essential for its homophilic adhesive properties in S2 cells. *J. Biol. Chem.* **270**, 18809-18817. doi:10.1074/jbc.270.32.18809

Hortsch, M., Nagaraj, K. and Godenschwege, T. (2009). The interaction between L1-type proteins and ankyrins–a master switch for L1-type CAM function. *Cell. Mol. Biol. Lett.* **14**, 57-69. doi:10.2478/s11658-008-0035-4

James, J. R., Oliveira, M. I., Carmo, A. M., Iaboni, A. and Davis, S. J. (2006). A rigorous experimental framework for detecting protein oligomerization using bioluminescence resonance energy transfer. *Nat. Methods* **3**, 1001-1006. doi:10.1038/nmeth978

Johnson, D. E., Drummond, E., Grimwood, S., Sawant-Basak, A., Miller, E., Tseng, E., McDowell, L. L., Vanase-Frawley, M. A., Fisher, K. E., Rubitski, D. M. et al. (2012). The 5-hydroxytryptamine$_4$ receptor agonists prucalopride and PRX-03140 increase acetylcholine and histamine levels in the rat prefrontal cortex and the power of stimulated hippocampal θ oscillations. *J. Pharmacol. Exp. Ther.* **341**, 681-691. doi:10.1124/jpet.112.192351

Kalus, I., Schnegelsberg, B., Seidah, N. G., Kleene, R. and Schachner, M. (2003). The proprotein convertase PC5A and a metalloprotease are involved in the proteolytic processing of the neural adhesion molecule L1. *J. Biol. Chem.* **278**, 10381-10388. doi:10.1074/jbc.M208351200

Kalus, I., Bormann, U., Mzoughi, M., Schachner, M. and Kleene, R. (2006). Proteolytic cleavage of the neural cell adhesion molecule by ADAM17/TACE is involved in neurite outgrowth. *J. Neurochem.* **98**, 78-88. doi:10.1111/j.1471-4159.2006.03847.x

Kenwrick, S., Watkins, A. and De Angelis, E. (2000). Neural cell recognition molecule L1: relating biological complexity to human disease mutations. *Hum. Mol. Genet.***9**, 879-886. doi:10.1093/hmg/9.6.879

Kleene, R., Chaudhary, H., Karl, N., Katic, J., Kotarska, A., Guitart, K., Loers, G. and Schachner, M. (2015). Interaction between CHL1 and serotonin receptor 2c regulates signal transduction and behavior in mice. *J. Cell Sci.* **128**, 4642-4652. doi:10.1242/jcs.176941

Kobe, F., Renner, U., Woehler, A., Wlodarczyk, J., Papusheva, E., Bao, G., Zeug, A., Richter, D. W., Neher, E. and Ponimaskin, E. (2008). Stimulation- and palmitoylation-dependent changes in oligomeric conformation of serotonin 5-HT1A receptorsi. *Biochim. Biophys. Acta (BBA) Mol. Cell Res.* **1783**, 1503-1516. doi:10.1016/j.bbamcr.2008.02.021

Kobe, F., Guseva, D., Jensen, T. P., Wirth, A., Renner, U., Hess, D., Muller, M., Medrihan, L., Zhang, W., Zhang, M. et al. (2012). 5-HT7R/G12 signaling regulates neuronal morphology and function in an age-dependent manner. *J. Neurosci.* **32**, 2915-2930. doi:10.1523/JNEUROSCI.2765-11.2012

Kozono, N., Ohtani, A. and Shiga, T. (2017). Roles of the serotonin 5-HT4 receptor in dendrite formation of the rat hippocampal neurons in vitro. *Brain Res.* **1655**, 114-121. doi:10.1016/j.brainres.2016.11.021

Kudumala, S., Freund, J., Hortsch, M. and Godenschwege, T. A. (2013). Differential effects of human L1CAM mutations on complementing guidance and synaptic defects in *Drosophila* melanogaster. *PLoS ONE* **8**, e76974. doi:10.1371/journal.pone.0076974

Kurumaji, A., Nomoto, H., Okano, T. and Toru, M. (2001). An association study between polymorphisms of L1CAM gene and schizophrenia in a Japanese sample. *Am. J. Med. Genet.* **105**, 99-104. doi:10.1002/1096-8628(20010108)105:1<99::AID-AJMG1071>3.0.CO;2-U

Laifenfeld, D., Karry, R., Grauer, E., Klein, E. and Ben-Shachar, D. (2005). Antidepressants and prolonged stress in rats modulate CAM-L1, laminin, and pCREB, implicated in neuronal plasticity. *Neurobiol. Dis.* **20**, 432-441. doi:10.1016/j.nbd.2005.03.023

Lemmon, V., Farr, K. L. and Lagenaur, C. (1989). L1-mediated axon outgrowth occurs via a homophilic binding mechanism. *Neuron* **2**, 1597-1603. doi:10.1016/0896-6273(89)90048-2

Li, X., Saint-Cyr-Proulx, E., Aktories, K. and Lamarche-Vane, N. (2002). Rac1 and Cdc42 but not RhoA or Rho kinase activities are required for neurite outgrowth induced by the Netrin-1 receptor DCC (deleted in colorectal cancer) in N1E-115 neuroblastoma cells. *J. Biol. Chem.* **277**, 15207-15214. doi:10.1074/jbc.M109913200

Lo, A. C., De Maeyer, J. H., Vermaercke, B., Callaerts-Vegh, Z., Schuurkes, J. A. J. and D'Hooge, R. (2014). SSP-002392, a new 5-HT4 receptor agonist, dose-dependently reverses scopolamine-induced learning and memory impairments in C57Bl/6 mice. *Neuropharmacology* **85**, 178-189. doi:10.1016/j.neuropharm.2014.05.013

Lucas, G., Rymar, V. V., Du, J., Mnie-Filali, O., Bisgaard, C., Manta, S., Lambas-Senas, L., Wiborg, O., Haddjeri, N., Piñeyro, G. et al. (2007). Serotonin$_4$ (5-HT$_4$) receptor agonists are putative antidepressants with a rapid onset of action. *Neuron* **55**, 712-725. doi:10.1016/j.neuron.2007.07.041

Lüthi, A., Laurent, J.-P., Figurov, A., Muller, D. and Schachner, M. (1994). Hippocampal long-term potentiation and neural cell adhesion molecules L1 and NCAM. *Nature* **372**, 777-779. doi:10.1038/372777a0

Lüthi, A., Mohajeri, H., Schachner, M. and Laurent, J.-P. (1996). Reduction of hippocampal long-term potentiation in transgenic mice ectopically expressing the neural cell adhesion molecule L1 in astrocytes. *J. Neurosci. Res.* **46**, 1-6. doi:10.1002/(SICI)1097-4547(19961001)46:1<1::AID-JNR1>3.0.CO;2-P

Lutz, D., Wolters-Eisfeld, G., Joshi, G., Djogo, N., Jakovcevski, I., Schachner, M. and Kleene, R. (2012). Generation and nuclear translocation of sumoylated transmembrane fragment of cell adhesion molecule L1. *J. Biol. Chem.* **287**, 17161-17175. doi:10.1074/jbc.M112.346759

Lutz, D., Loers, G., Kleene, R., Oezen, I., Kataria, H., Katagihallimath, N., Braren, I., Harauz, G. and Schachner, M. (2014a). Myelin basic protein cleaves cell adhesion molecule L1 and promotes neuritogenesis and cell survival. *J. Biol. Chem.* **289**, 13503-13518. doi:10.1074/jbc.M113.530238

Lutz, D., Wolters-Eisfeld, G., Schachner, M. and Kleene, R. (2014b). Cathepsin E generates a sumoylated intracellular fragment of the cell adhesion molecule L1 to promote neuronal and Schwann cell migration as well as myelination. *J. Neurochem.* **128**, 713-724. doi:10.1111/jnc.12473

Lutz, D., Sharaf, A., Drexler, D., Kataria, H., Wolters-Eisfeld, G., Brunne, B., Kleene, R., Loers, G., Frotscher, M. and Schachner, M. (2017). Proteolytic cleavage of transmembrane cell adhesion molecule L1 by extracellular matrix molecule Reelin is important for mouse brain development. *Sci. Rep.* **7**, 15268. doi:10.1038/s41598-017-15311-x

Maillet, M., Robert, S. J., Cacquevel, M., Gastineau, M., Vivien, D., Bertoglio, J., Zugaza, J. L., Fischmeister, R. and Lezoualc'h, F. (2003). Crosstalk between Rap1 and Rac regulates secretion of sAPPα. *Nat. Cell Biol.* **5**, 633-639. doi:10.1038/ncb1007

Maness, P. F. and Schachner, M. (2007). Neural recognition molecules of the immunoglobulin superfamily: signaling transducers of axon guidance and neuronal migration. *Nat. Neurosci.* **10**, 19-26. doi:10.1038/nn1827

Manzke, T., Guenther, U., Ponimaskin, E. G., Haller, M., Dutschmann, M., Schwarzacher, S. and Richter, D. W. (2003). 5-HT4(a) receptors avert opioid-induced breathing depression without loss of analgesia. *Science* **301**, 226-229. doi:10.1126/science.1084674

Marchetti, E., Jacquet, M., Escoffier, G., Miglioratti, M., Dumuis, A., Bockaert, J. and Roman, F. S. (2011). Enhancement of reference memory in aged rats by specific activation of 5-HT$_4$ receptors using an olfactory associative discrimination task. *Brain Res.* **1405**, 49-56. doi:10.1016/j.brainres.2011.06.020

Maretzky, T., Schulte, M., Ludwig, A., Rose-John, S., Blobel, C., Hartmann, D., Altevogt, P., Saftig, P. and Reiss, K. (2005). L1 is sequentially processed by two differently activated metalloproteases and presenilin/γ-secretase and regulates neural cell adhesion, cell migration, and neurite outgrowth. *Mol. Cell. Biol.* **25**, 9040-9053. doi:10.1128/MCB.25.20.9040-9053.2005

Matsumoto-Miyai, K., Ninomiya, A., Yamasaki, H., Tamura, H., Nakamura, Y. and Shiosaka, S. (2003). NMDA-dependent proteolysis of presynaptic adhesion molecule L1 in the hippocampus by neuropsin. *J. Neurosci.* **23**, 7727-7736. doi:10.1523/JNEUROSCI.23-21-07727.2003

Mawe, G. M. and Hoffman, J. M. (2013). Serotonin signalling in the gut—functions, dysfunctions and therapeutic targets. *Nat. Rev. Gastroenterol. Hepatol.* **10**, 473-486. doi:10.1038/nrgastro.2013.105

Mechtersheimer, S., Gutwein, P., Agmon-Levin, N., Stoeck, A., Oleszewski, M., Riedle, S., Postina, R., Fahrenholz, F., Fogel, M., Lemmon, V. et al. (2001). Ectodomain shedding of L1 adhesion molecule promotes cell migration by autocrine binding to integrins. *J. Cell Biol.* **155**, 661-673. doi:10.1083/jcb.200101099

Meyer, B. H., Segura, J.-M., Martinez, K. L., Hovius, R., George, N., Johnsson, K. and Vogel, H. (2006). FRET imaging reveals that functional neurokinin-1 receptors are monomeric and reside in membrane microdomains of live cells. *Proc. Natl. Acad. Sci. USA* **103**, 2138-2143. doi:10.1073/pnas.0507686103

Milev, P., Friedlander, D. R., Sakurai, T., Karthikeyan, L., Flad, M., Margolis, R. K., Grumet, M. and Margolis, R. U. (1994). Interactions of the chondroitin sulfate proteoglycan phosphacan, the extracellular domain of a receptor-type protein tyrosine phosphatase, with neurons, glia, and neural cell adhesion molecules. *J. Cell Biol.* **127**, 1703-1715. doi:10.1083/jcb.127.6.1703

Moon, M.-S. and Gomez, T. M. (2010). Balanced Vav2 GEF activity regulates neurite outgrowth and branching in vitro and in vivo. *Mol. Cell. Neurosci.* **44**, 118-128. doi:10.1016/j.mcn.2010.03.001

Moos, M., Tacke, R., Scherer, H., Teplow, D., Früh, K. and Schachner, M. (1988). Neural adhesion molecule L1 as a member of the immunoglobulin superfamily with binding domains similar to fibronectin. *Nature* **334**, 701-703. doi:10.1038/334701a0

Müller, P. and Cunningham, K. A. (2020). *Handbook of the Behavioral Neurobiology of Serotonin*. Elsevier.

Nayeem, N., Silletti, S., Yang, X., Lemmon, V. P., Reisfeld, R. A., Stallcup, W. B. and Montgomery, A. M. (1999). A potential role for the plasmin(ogen) system in the posttranslational cleavage of the neural cell adhesion molecule L1. *J. Cell Sci.* **112**, 4739-4749.

Niebert, S., van Belle, G. J., Vogelgesang, S., Manzke, T. and Niebert, M. (2017). The serotonin receptor subtype 5b specifically Interacts with serotonin Receptor subtype 1A. *Front. Mol. Neurosci.* **10**, 299. doi:10.3389/fnmol.2017.00299

Niwa, R., Nagata-Ohashi, K., Takeichi, M., Mizuno, K. and Uemura, T. (2002). Control of actin reorganization by slingshot, a family of phosphatases that dephosphorylate ADF/cofilin. *Cell* **108**, 233-246. doi:10.1016/S0092-8674(01)00638-9

Nordman, J. C. and Kabbani, N. (2014). Microtubule dynamics at the growth cone are mediated by α7 nicotinic receptor activation of a Gαq and IP$_3$ receptor pathway. *FASEB J.* **28**, 2995-3006. doi:10.1096/fj.14-251439

Norum, J. H., Hart, K. and Levy, F. O. (2003). Ras-dependent ERK activation by the human G$_s$-coupled serotonin receptors 5-HT$_{4(b)}$ and 5-HT$_{7(a)}$. *J. Biol. Chem.* **278**, 3098-3104. doi:10.1074/jbc.M206237200

Patzke, C., Acuna, C., Giam, L. R., Wernig, M. and Südhof, T. C. (2016). Conditional deletion of L1CAM in human neurons impairs both axonal and dendritic arborization and action potential generation. *J. Exp. Med.* **213**, 499-515. doi:10.1084/jem.20150951

Pellissier, L. P., Barthet, G., Gaven, F., Cassier, E., Trinquet, E., Pin, J.-P., Marin, P., Dumuis, A., Bockaert, J., Banères, J.-L. et al. (2011). G protein activation by serotonin type 4 receptor dimers: evidence that turning on two protomers is more efficient. *J. Biol. Chem.* **286**, 9985-9997. doi:10.1074/jbc.M110.201939

Ponimaskin, E. G., Profirovic, J., Vaiskunaite, R., Richter, D. W. and Voyno-Yasenetskaya, T. A. (2002). 5-Hydroxytryptamine 4(a) receptor is coupled to the Gα subunit of heterotrimeric G$_{13}$ protein. *J. Biol. Chem.* **277**, 20812-20819. doi:10.1074/jbc.M112216200

Prasad, S., Zeug, A. and Ponimaskin, E. (2013). Analysis of receptor-receptor interaction by combined application of FRET and microscopy. *Methods Cell Biol.* **117**, 243-265. doi:10.1016/B978-0-12-408143-7.00014-1

Renner, U., Zeug, A., Woehler, A., Niebert, M., Dityatev, A., Dityateva, G., Gorinski, N., Guseva, D., Abdel-Galil, D., Frohlich, M. et al. (2012). Heterodimerization of serotonin receptors 5-HT1A and 5-HT7 differentially regulates receptor signalling and trafficking. *J. Cell Sci.* **125**, 2486-2499. doi:10.1242/jcs.101337

Riedle, S., Kiefel, H., Gast, D., Bondong, S., Wolterink, S., Gutwein, P. and Altevogt, P. (2009). Nuclear translocation and signalling of L1-CAM in human carcinoma cells requires ADAM10 and presenilin/γ-secretase activity. *Biochem. J.* **420**, 391-402. doi:10.1042/BJ20081625

Roonprapunt, C., Huang, W., Grill, R., Friedlander, D., Grumet, M., Chen, S., Schachner, M. and Young, W. (2003). Soluble cell adhesion molecule L1-Fc promotes locomotor recovery in rats after spinal cord injury. *J. Neurotrauma* **20**, 871-882. doi:10.1089/089771503322385809

Sadoul, K., Sadoul, R., Faissner, A. and Schachner, M. (1988). Biochemical characterization of different molecular forms of the neural cell adhesion molecule L1. *J. Neurochem.* **50**, 510-521. doi:10.1111/j.1471-4159.1988.tb02941.x

Salzberg, Y., Díaz-Balzac, C. A., Ramirez-Suarez, N. J., Attreed, M., Tecle, E., Desbois, M., Kaprielian, Z. and Bülow, H. E. (2013). Skin-derived cues control arborization of sensory dendrites in Caenorhabditis elegans. *Cell* **155**, 308-320. doi:10.1016/j.cell.2013.08.058

Sandi, C. and Bisaz, R. (2007). A model for the involvement of neural cell adhesion molecules in stress-related mood disorders. *Neuroendocrinology* **85**, 158-176. doi:10.1159/000101535

Schaefer, A. W., Kamei, Y., Kamiguchi, H., Wong, E. V., Rapoport, I., Kirchhausen, T., Beach, C. M., Landreth, G., Lemmon, S. K and Lemmon, V. (2002). L1 endocytosis is controlled by a phosphorylation-dephosphorylation cycle stimulated by outside-in signaling by L1. *J. Cell Biol.* **157**, 1223-1232. doi:10.1083/jcb.200203024

Schill, Y., Bijata, M., Kopach, O., Cherkas, V., Abdel-Galil, D., Böhm, K., Schwab, M. H., Matsuda, M., Compan, V., Basu, S. et al. (2020). Serotonin 5-HT4 receptor boosts functional maturation of dendritic spines via RhoA-dependent control of F-actin. *Commun. Biol.* **3**, 76. doi:10.1038/s42003-020-0791-x

Schmid, R. S. and Maness, P. F. (2008). L1 and NCAM adhesion molecules as signaling coreceptors in neuronal migration and process outgrowth. *Curr. Opin. Neurobiol.* **18**, 245-250. doi:10.1016/j.conb.2008.07.015

Schmid, R.-S., Pruitt, W. M. and Maness, P. F. (2000). A MAP kinase-signaling pathway mediates neurite outgrowth on L1 and requires Src-dependent endocytosis. *J. Neurosci.* **20**, 4177-4188. doi:10.1523/JNEUROSCI.20-11-04177.2000

Schmid, R. S., Midkiff, B. R., Kedar, V. P. and Maness, P. F. (2004). Adhesion molecule L1 stimulates neuronal migration through Vav2-Pak1 signaling. *Neuroreport* **15**, 2791-2794.

Schmidt, A. and Hall, A. (2002). Guanine nucleotide exchange factors for Rho GTPases: turning on the switch. *Genes Dev.* **16**, 1587-1609. doi:10.1101/gad.1003302

Swenson-Fields, K. I., Sandquist, J. C., Rossol-Allison, J., Blat, I. C., Wennerberg, K., Burridge, K. and Means, A. R. (2008). MLK3 limits activated Gαq signaling to Rho by binding to p63RhoGEF. *Mol. Cell* **32**, 43-56. doi:10.1016/j.molcel.2008.09.007

Sytnyk, V., Leshchyns'ka, I. and Schachner, M. (2017). Neural cell adhesion molecules of the immunoglobulin superfamily regulate synapse formation, maintenance, and function. *Trends Neurosci.* **40**, 295-308. doi:10.1016/j.tins.2017.03.003

Toshima, J., Toshima, J. Y., Amano, T., Yang, N., Narumiya, S. and Mizuno, K. (2001a). Cofilin phosphorylation by protein kinase testicular protein kinase 1 and its role in integrin-mediated actin reorganization and focal adhesion formation. *Mol. Biol. Cell* **12**, 1131-1145. doi:10.1091/mbc.12.4.1131

Toshima, J., Toshima, J. Y., Takeuchi, K., Mori, R. and Mizuno, K. (2001b). Cofilin phosphorylation and actin reorganization activities of testicular protein kinase 2 and its predominant expression in testicular Sertoli cells. *J. Biol. Chem.* **276**, 31449-31458. doi:10.1074/jbc.M102988200

Van Gijsegem, F., Wlodarczyk, A., Cornu, A., Reverchon, S. and Hugouvieux-Cotte-Pattat, N. (2008). Analysis of the LacI family regulators of Erwinia chrysanthemi 3937, involvement in the bacterial phytopathogenicity. *Mol. Plant-Microbe Interact.* **21**, 1471-1481. doi:10.1094/MPMI-21-11-1471

Wirth, A., Holst, K. and Ponimaskin, E. (2017). How serotonin receptors regulate morphogenic signalling in neurons. *Prog. Neurobiol.* **151**, 35-56. doi:10.1016/j.pneurobio.2016.03.007

Wlodarczyk, J., Woehler, A., Kobe, F., Ponimaskin, E., Zeug, A. and Neher, E. (2008). Analysis of FRET signals in the presence of free donors and acceptors. *Biophys. J.* **94**, 986-1000. doi:10.1529/biophysj.107.111773

Wong, E. V., Cheng, G., Payne, H. R. and Lemmon, V. (1995). The cytoplasmic domain of the cell adhesion molecule L1 is not required for homophilic adhesion. *Neurosci. Lett.* **200**, 155-158. doi:10.1016/0304-3940(95)12100-I

Yang, N., Higuchi, O., Ohashi, K., Nagata, K., Wada, A., Kangawa, K., Nishida, E. and Mizuno, K. (1998). Cofilin phosphorylation by LIM-kinase 1 and its role in Rac-mediated actin reorganization. *Nature* **393**, 809-812. doi:10.1038/31735

Zeug, A., Woehler, A., Neher, E. and Ponimaskin, E. G. (2012). Quantitative intensity-based FRET approaches—a comparative snapshot. *Biophys. J.* **103**, 1821-1827. doi:10.1016/j.bpj.2012.09.031

Zhang, Y., Bo, X., Schoepfer, R., Holtmaat, A. J. D. G., Verhaagen, J., Emson, P. C., Lieberman, A. R. and Anderson, P. N. (2005). Growth-associated protein GAP-43 and L1 act synergistically to promote regenerative growth of Purkinje cell axons in vivo. *Proc. Natl. Acad. Sci. USA* **102**, 14883-14888. doi:10.1073/pnas.0505164102

Zhao, X. and Siu, C.-H. (1995). Colocalization of the homophilic binding site and the neuritogenic activity of the cell adhesion molecule L1 to its second Ig-like domain. *J. Biol. Chem.* **270**, 29413-29421. doi:10.1074/jbc.270.49.29413